Rendiconti Lincei. Scienze Fisiche e Naturali
https://doi.org/10.1007/s12210-024-01290-5

MINERALS AS TREASURE TROVE FOR SCIENTIFIC DISCOVERIES

Decavanadates and polyanion-polycation interactions: from minerals to proteins

Frank C. Hawthorne[1]

Received: 4 September 2024 / Accepted: 16 November 2024

Abstract
The decavanadate polyanions $[V_{10}O_{28}]^{6-}$, $[H_xV_{10}O_{28}]^{(6-x)-}$ and $[(M^{4+}{}_xV^{5+}{}_{10-x})O_{28}]^{(6+x)-}$ are constituents of the pascoite-family minerals. The interaction between the *interstitial complex* and the decavanadate *structural unit* may be analyzed using the principle of correspondence of Lewis acidity-basicity. The Lewis base strengths of the decavanadate polyanions vary from 0.054 to 0.135 *vu* and $[V_{10}O_{28}]$ structures can form from Cs^+, Rb^+, K^+, Tl^+ and Na^+; simple cations with higher Lewis acidities are too acidic to form structures. Such cations bond to transformer (H_2O) groups to form polyatomic cations that have lower Lewis acidities than the corresponding simple cations. In the pascoite-family minerals, the stereochemical details of the decavanadate ion are modified by (1) exploiting the two different patterns of bond-length arrangement in $^{[6]}V^{5+}$, (2) substituting tetravalent cations for V^{5+} at one of the octahedra, and (3) protonating the decavanadate ion. These mechanisms change the individual Lewis basicities of the 26 external O^{2-} ions of the polyanion, allowing great versatility in the binding of decavanadate ions to constituent polycations of crystallizing structures. This suggests that the $[V_{10}O_{28}]$ polyanions may be used to induce co-crystallization of large aqueous polyatomic cations, facilitating their structural characterization. Decavanadate can also induce crystallization of proteins and is of major importance in protein crystallography because of this capability. Proteins and enzymes can bind to the decavanadate ion as very large polyatomic cations, modifying their function and showing potential for treating various forms of cancer, Alzheimer's disease, AIDS, diabetes and COVID-19.

Keywords Decavanadate · Lewis acidity-basicity · Pascoite-family minerals · Interstitial polyanions · Proteins · Enzymes

1 Introduction

Polyoxidometalates are a group of compounds that contain clusters of three or more transition-metal ions from group 5 and group 6 of the Periodic Table. These ions are in their high oxidation states, d^0 and d^1 configurations, e.g., (V^{5+}, Nb^{5+}, Ta^{5+}) and (Mo^{6+} and W^{6+}), and occur as transition-metal-centered polyhedra that are linked together by sharing O^{2-} ions between the polyhedra. Synthetic polyoxidometalate compounds have many important industrial applications: coatings, gas sorbents, sensors, dyes, capacitors, cation exchangers, nanomagnetism and semiconductors (see the excellent review by Katsoulis 1998), and medical applications as potential anti-tumor agents (e.g., Aureliano et al. 2021), antiviral agents (e.g., Bijelic et al. 2018), treatment of AIDS and Covid (e.g., Lentink et al. 2023) and cancer antagonists (e.g., Bijelic et al. 2019).

The Uravan Mineral Belt is a 120-km-long region of roll-front uranium-vanadium deposits in the Salt Wash sandstone of the Morrison Formation (Carter and Gualtieri 1965; Shawe 2011) on the Colorado Plateau of western Colorado and eastern Utah, USA. Mines within this belt have been a productive source of U and V ores during the twentieth century. Detailed investigation of post-mining secondary minerals in this region pioneered by Tony Kampf has resulted in the discovery of many new polyoxidometalate minerals. The most common polyoxidometalate minerals from the Colorado Plateau belong to the pascoite family (Table 1) and involve the decavanadate polyanions $[V_{10}O_{28}]^{6-}$, $[H_xV_{10}O_{28}]^{(6-x)-}$ and $[(M^{4+}{}_xV^{5+}{}_{10-x})O_{28}]^{(6+x)-}$. Since 2008,

This paper is part of the Topical Collection "Minerals as treasure trove for scientific discoveries" originated from the international and interdisciplinary meeting held at the Accademia Nazionale dei Lincei in Rome on February 14-15, 2024.

✉ Frank C. Hawthorne
frank.hawthorne@umanitoba.ca

[1] Earth Sciences, University of Manitoba, Winnipeg, MB R3T 2N2, Canada

Published online: 05 December 2024

Table 1 Minerals of the pascoite family

Mineral species	Ideal formula	First references; structure references
Decavanadates: $[V_{10}O_{28}]^{6-}$		
Ammoniolasalite	$(NH_4)_2Mg_2[V_{10}O_{28}](H_2O)_{20}$	Kampf et al. 2018
Burroite	$(NH_4)_2Ca_2[V_{10}O_{28}](H_2O)_{15}$	Kampf et al. 2017a
Gunterite	$Na_2Ca_2[V_{10}O_{28}](H_2O)_{22}$	Kampf et al. 2011a, 2022a
Huemulite	$Na_4Mg[V_{10}O_{28}](H_2O)_{24}$	Gordillo et al. 1966; Colombo et al. 2011
Hughesite	$Na_3Al[V_{10}O_{28}](H_2O)_{22}$	Rakovan et al. 2011
Hummerite	$K_2Mg_2[V_{10}O_{28}](H_2O)_{16}$	Weeks et al. 1951; Hughes et al. 2002
Hydropascoite	$Ca_3[V_{10}O_{28}](H_2O)_{24}$	Kampf et al. 2017b
Kokinosite	$Na_2Ca_2[V_{10}O_{28}](H_2O)_{24}$	Kampf et al. 2014a
Lasalite	$Na_2Mg_2[V_{10}O_{28}](H_2O)_{20}$	Hughes et al. 2008
Magnesiopascoite	$Ca_2Mg[V_{10}O_{28}](H_2O)_{16}$	Kampf and Steele 2008
Okieite	$Mg_3[V_{10}O_{28}](H_2O)_{28}$	Kampf et al. 2020b
Pascoite	$Ca_3[V_{10}O_{28}](H_2O)_{17}$	Hillebrand et al. 1914; Hughes et al. 2005
Postite	$MgAl_2(OH)_2[V_{10}O_{28}](H_2O)_{27}$	Kampf et al. 2012
Protocaseyite	$[Al_4(OH)_6(H_2O)_{12}][V_{10}O_{28}](H_2O)_8$	Kampf et al. 2022b
Rakovanite	$(NH_4)_3Na_3[V_{10}O_{28}](H_2O)_{12}$	Kampf et al. 2011b; Kampf et al. 2021
Schindlerite	$(NH_4)_4Na_2[V_{10}O_{28}](H_2O)_{10}$	Kampf et al. 2013a; Kampf et al. 2016
Wernerbaurite	$(NH_4)_2Ca_2[V_{10}O_{28}](H_2O)_{16}$	Kampf et al. 2013a; Kampf et al. 2016
Bluestreakite	$K_4Mg_2[(V^{4+}{}_2V^{5+}{}_8)O_{28}](H_2O)_{14}$	Kampf et al. 2014b
Nashite	$Na_3Ca_2[(V^{4+}V^{5+}{}_9)O_{28}](H_2O)_{24}$	Kampf et al. 2013b
Trebiskyite	$Na_3Mg_2[(Ti^{4+}V^{5+}{}_9)O_{28}](H_2O)_{22}$	Olds et al. 2024
Hydrogenated mixed-valence decavanadates: $[H_n(M^{4+}{}_x,V^{5+}{}_{(1-x)})_{10}O_{28}]^{6-n}$		
Caseyite	$[(V^{5+}O_2)Al_{7.5}(OH)_{15}(H_2O)_{13}]_2$ $[H_2(V^{4+}V^{5+}{}_9)O_{28}][V^{5+}{}_{10}O_{28}]_2(H_2O)_{90}$	Kampf et al. 2020a

the number of minerals in this family has increased from 3 to 21.

2 The pascoite-family minerals

The minerals of the pascoite family are based on the decavanadate polyanion, the simplest form of which is the $[V^{5+}{}_{10}O_{28}]^{6-}$ group. Inspection of Table 1 shows that $[V^{5+}{}_{10}O_{28}]^{6-}$ is by far the most common form of decavanadate in these minerals but more complex (sensu lato) forms also occur. The general form of the chemical formulae consists of a decavanadate polyanion (shown in green in Fig. 1) which is the *structural unit* (Hawthorne 1983, 2014) and an array of lower-valence cations plus (H_2O) groups that forms the *interstitial complex* (Hawthorne 1983, 2014). These features are illustrated for pascoite in Fig. 1. Stereochemical details of the $[V^{5+}{}_{10}O_{28}]^{6-}$ decavanadate group are shown in Fig. 2 using the nomenclature of Schindler et al. (2000a, b) and Cooper et al. (2019a, b). The decavanadate unit ideally has 2/*m*2/*m*2/*m* symmetry, and it is generally assumed that the free polyanion has this symmetry (Evans 1966) and that deviations arise from the influence of neighboring ions and groups both in crystals and in aqueous solution. As indicated in Fig. 2, there is considerable variation in coordination number for the O^{2-} ions of the decavanadate group, and this variation plays a key role in the adaptability of the group to a wide variety of constituents that can form the interstitial complex of the complete structures.

3 Binary structure representation, Lewis basicity and Lewis acidity

This partitioning of a complicated crystal structure into two parts is known as *binary structure representation* (Hawthorne 2012, 2015): a complicated structure is considered as two components, a strongly bonded (usually anionic) *structural unit* and a weakly bonded (usually cationic) *interstitial complex* (Hawthorne 1983), and the bonding between these two components may be quantitatively characterized using Lewis-acid–Lewis-base interactions (Fig. 3). The *Lewis-acid strength* of a cation is defined as the characteristic valence (strength) of the bonds formed by that cation (Brown 2016), and values are given by Gagné and Hawthorne (2017) as the oxidation state of a cation divided by its *characteristic coordination number*,

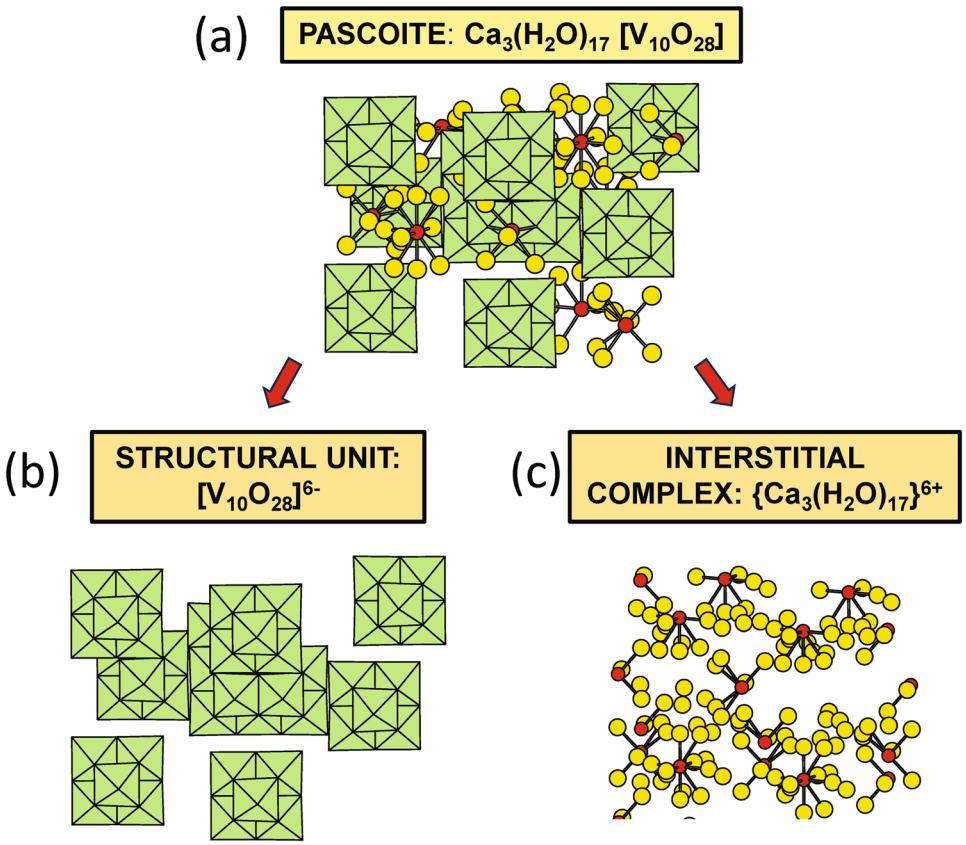

Fig. 1 The crystal structure of pascoite; **a** shows the complete structure, **b** shows the structural unit, and **c** shows the interstitial complex. ($V^{5+}O_6$) octahedra are shaded green, Ca^{2+} ions are shown as red circles and O^{2-} ions are shown as yellow circles; H^+ ions are omitted for clarity

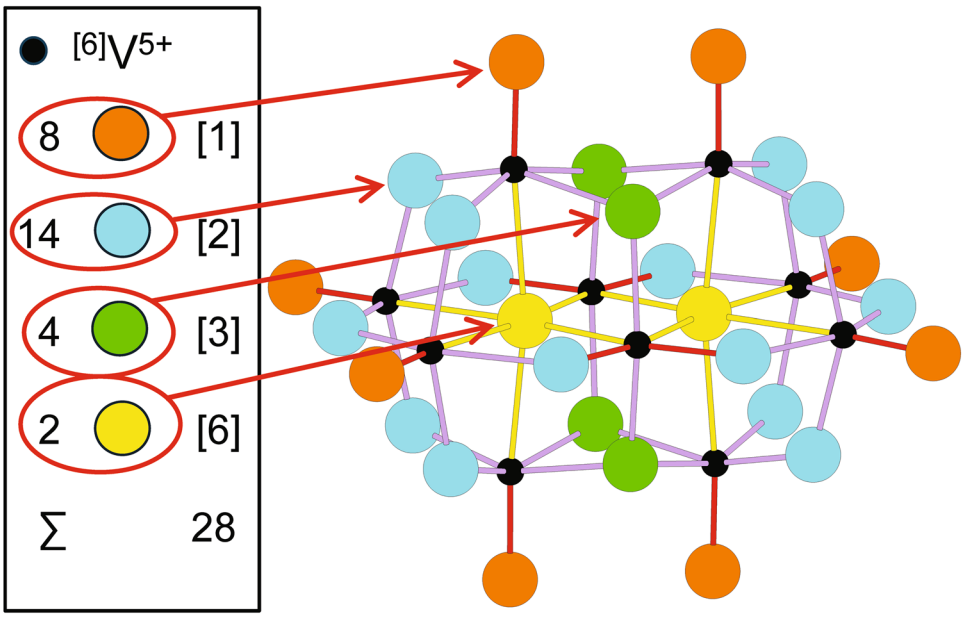

Fig. 2 The $[V_{10}O_{28}]^{6-}$ decavanadate polyanion. V atoms = black circles, [1]-coordinated O atoms = brown circles, [2]-coordinated O atoms = blue circles, [3]-coordinated O atoms = green circles, [6]-coordinated O atoms = yellow circles, V–$O_{vanadyl}$ bonds = red lines, V–O_{trans} bonds = yellow lines, V–$O_{equatorial}$ bonds = mauve lines

the *weighted grand-mean coordination number* given by Gagné and Hawthorne (2016, 2018a, 2018b, 2020) and Hawthorne and Gagné (2024) for each oxidation state of each cation in the periodic table; these values are used here. Lewis-base strengths for simple anions show too large a range in variation to be useful in examining chemical compositions and bond topologies of crystal structures. Simple oxyanions, e.g., $(SO_4)^{2-}$, $(SiO_4)^{4-}$, show a much

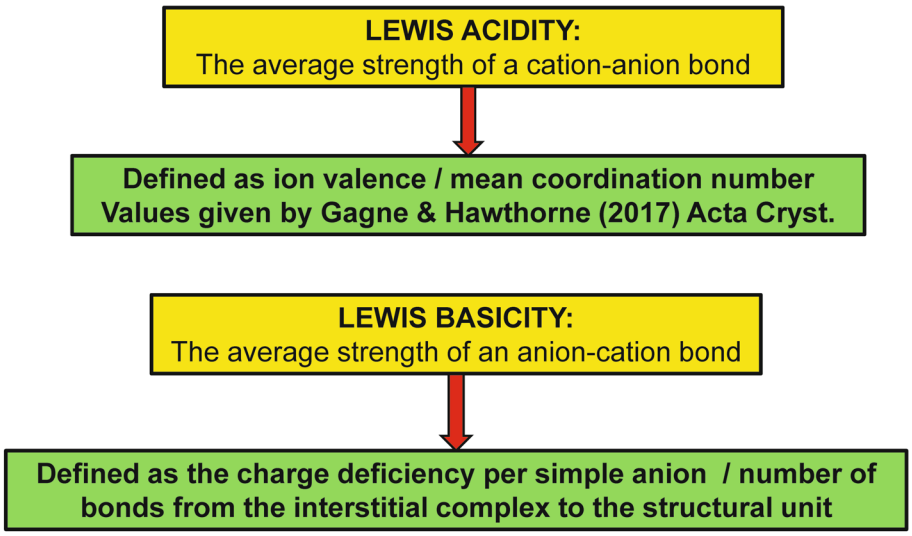

Fig. 3 Definitions of Lewis acidity and Lewis basicity

more limited variation (e.g., Brown 2009; Hawthorne 2012), and Lewis base strengths used here are from Hawthorne (2018).

3.1 The valence-matching principle

The interaction of structural units and interstitial complexes may be examined using the *valence-matching principle*: stable structures will form where the Lewis-acid strength of the cation closely matches the Lewis-base strength of the anion (Brown 2016; Hawthorne and Schindler 2008; Schindler and Hawthorne 2001a, 2001b, 2008). This principal is extremely powerful as it allows us to examine interaction of structural unit and interstitial complex without knowing the details of the crystal structure.

Let us consider three simple examples taken from Hawthorne (1994). Consider Na_2SO_4: the Lewis basicity of the (SO_4) group is 0.17 *vu* and the Lewis acidity of Na is 0.17 *vu*. The Lewis basicity of the anion matches the Lewis acidity of the cation, the valence-matching principle is satisfied, Na_2SO_4 is stable and corresponds to thenardite (Hawthorne and Ferguson 1975). Consider Na_4SiO_4. The Lewis basicity of the (SiO_4) group is 0.33 *vu* and the Lewis acidity of Na is 0.17 *vu.* The Lewis basicity of the anion does not match the Lewis acidity of the cation, the valence-matching principle is not satisfied, and Na_4SiO_4 is not a mineral. Consider $Na[AlSiO_4]$. The Lewis basicity of the $[AlSiO_4]$ group is 0.13 *vu* and the Lewis acidity of Na is 0.17 *vu*. The Lewis basicity of the anion approximately matches the Lewis acidity of the cation, the valence-matching principle is satisfied, and $NaAlSiO_4$ corresponds to nepheline (e.g., Tait et al. 2003). Nepheline shows incommensurate behavior (e.g., Angel et al. 2008), reflecting the minor mismatch between the basicity and acidity of its constituents.

3.2 The principle of correspondence of Lewis acidity-basicity

The valence-matching principle deals with single ion-ion interactions. However, in more complicated minerals such as those of the pascoite family (Table 1), the structural unit and the interstitial complex are complicated aggregations of ions and neutral species. We may define a Lewis basicity for a structural unit and a Lewis acidity for an interstitial complex and look at the aggregate interaction between these units (Fig. 4) using the *principle of correspondence of Lewis acidity-basicity* (Hawthorne and Schindler 2008), a mean-field equivalent of the valence-matching principle (Hawthorne 2012, 2015).

4 Polyoxidometallic ions

The decavanadate ion is a *polyoxidometalate* (or *POM*), a polyatomic ion that consists of three or more transition-metal polyhedra linked by shared O^{2-} ions to form dense packings of oxo-polyhedra. The metal atoms are group 5 (V, Nb, Ta), group 6 (Mo, W) and group 7 (Tc, Re) transition-metals in their high oxidation states. With regard to their interaction with simple cations, polycations and neutral species, V^{5+},

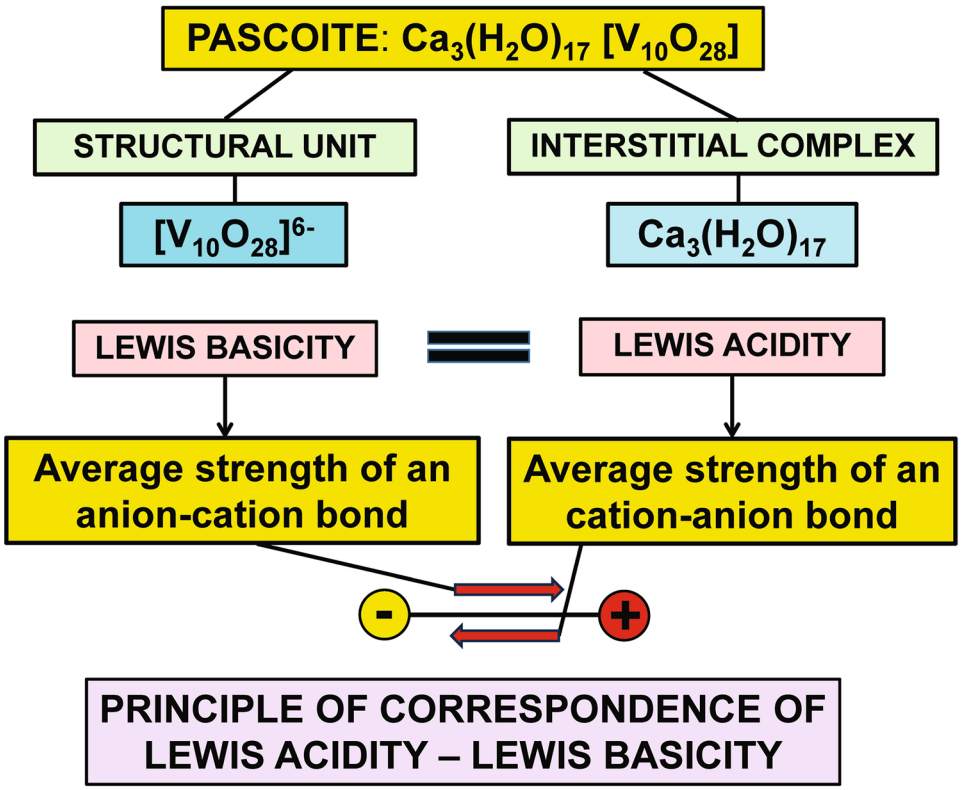

Fig. 4 The principle of correspondence of Lewis acidity – Lewis basicity applied to the structure of pascoite

Mo^{6+} and W^{6+} are particularly effective in this regard and examination of their general bond-length distributions tells us why. Figure 5 shows the variation in bond lengths for $^{[6]}V^{5+}$, $^{[6]}Mo^{6+}$ and $^{[6]}W^{6+}$. They all have strongly trimodal distributions but $^{[6]}Mo^{6+}$ and $^{[6]}W^{6+}$ have frequencies of 2:2:2 whereas $^{[6]}V^{5+}$ is more irregular. This less well-defined trimodal behaviour arises because $^{[6]}V^{5+}$–O octahedra can adopt two different configurations. As shown in Fig. 6a, one type of octahedron has two short V–O bonds in the range 1.5–1.7 Å that are known as *vanadyl* bonds and are adjacent to each other. There are two long V–O bonds in the range 2.1–2.2 Å; these bonds are *trans* to the vanadyl bonds and are known as *trans* bonds. The octahedron is completed by two V–O bonds of intermediate length 1.9–2.0 Å that occur approximately orthogonal to the plane of the vanadyl and *trans* bonds and are known as *equatorial* bonds. This type of configuration is denoted as [2 + 2 + 2]. As shown in Fig. 6b, the other type of octahedron has one vanadyl bond and one *trans* bond in the range 2.0–2.6 Å, and four equatorial bonds approximately orthogonal to the direction of the vanadyl and *trans* bonds. This type of configuration is denoted as [1 + 4 + 1]. The mean bond-lengths of the different types of bonds in the two types of decavanadate octahedra are shown in Fig. 7. The two different types of coordination result in a more irregular overall variation in the distribution of bond lengths than occurs for $^{[6]}Mo^{6+}$ and $^{[6]}W^{6+}$ (Fig. 5). In the decavanadates, this flexibility in bond lengths for $^{[6]}V^{5+}$ combines with the variation in coordination number of the O^{2-} ions of the decavanadate unit (Fig. 2) to produce a polyoxidometallic ion that can combine with a wide variety of counterions, accounting for the diverse nature of the interstitial complex in decavanadate structures.

5 The decavanadate groups

5.1 The undecorated $[V^{5+}{}_{10}O_{28}]^{6-}$ decavanadate polyanion

The decavanadate group consists of ten (VO_6) octahedra that share edges to form a closely packed polyanion of maximum symmetry 2/*m*2/*m*2/*m* with the inversion centre between V1 and V10 in Fig. 2. However, in most crystal structures, the symmetry of the decavanadate group is significantly lower due to the influence of the interstitial complex on the overall structure. The $[V^{5+}{}_{10}O_{28}]^{6-}$ polyanion shown in Fig. 2 may be decorated by H^+ ions and modified by replacement of (usually one) V^{5+} ion by a different ion (e.g., V^{4+}, Ti^{4+}), but the undecorated $[V^{5+}{}_{10}O_{28}]^{6-}$ polyanion is by far the most common structural unit in the pascoite-family of minerals (Table 1). Due to the compact nature of the group, there is wide variation in the coordination numbers of the various O^{2-} ions (Fig. 2). In the centre of the group, there are two [6]-coordinated O^{2-} ions (shown as yellow circles in Fig. 2);

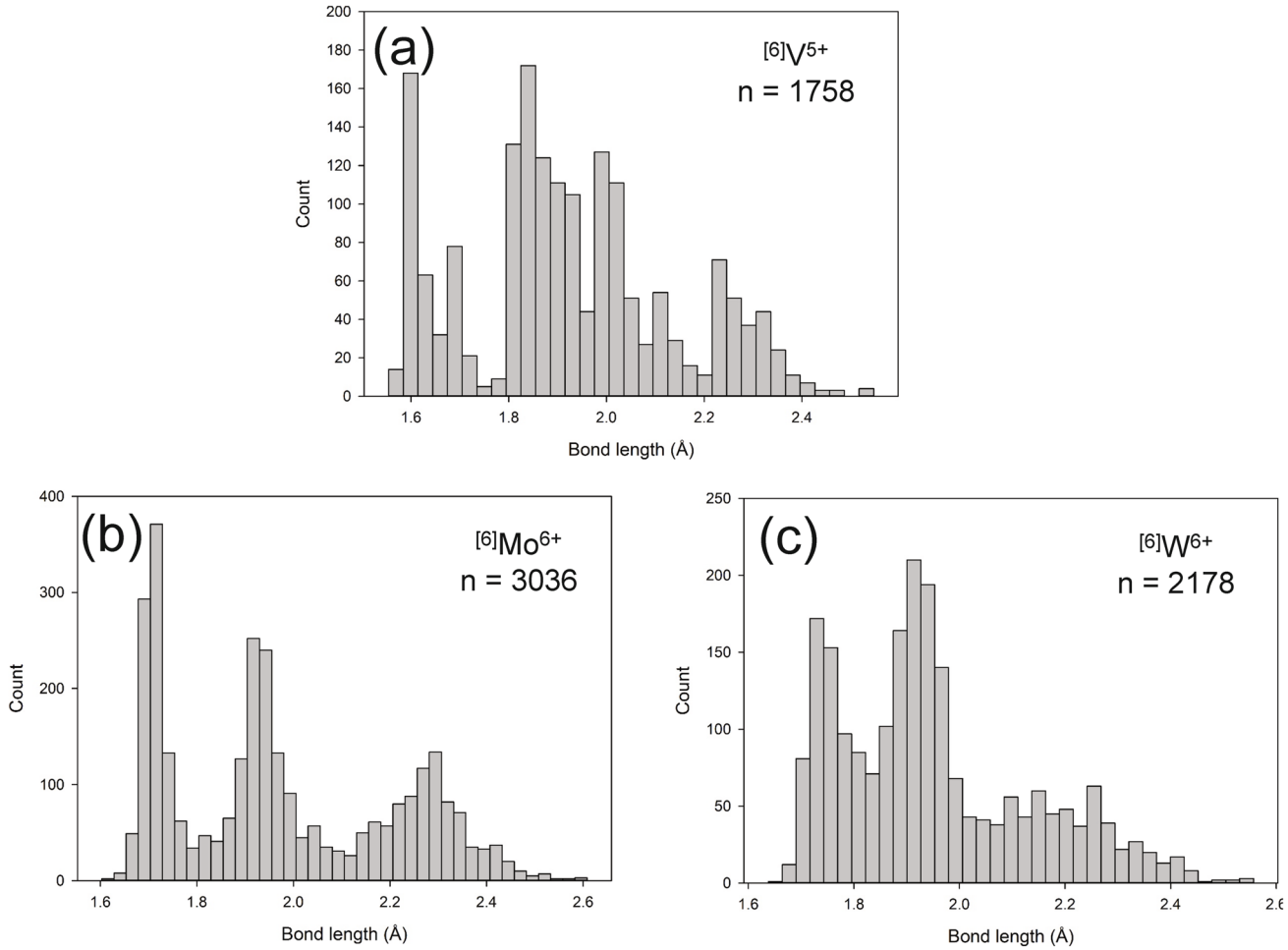

Fig. 5 Variation in bond lengths for ions commonly forming polyoxidometallic ions: **a** $^{[6]}V^{5+}$–O^{2-}; **b** $^{[6]}Mo^{6+}$–O^{2-}; **c** $^{[6]}W^{6+}$–$O.^{2-}$; n = number of bond lengths included; after Gagné and Hawthorne (2020)

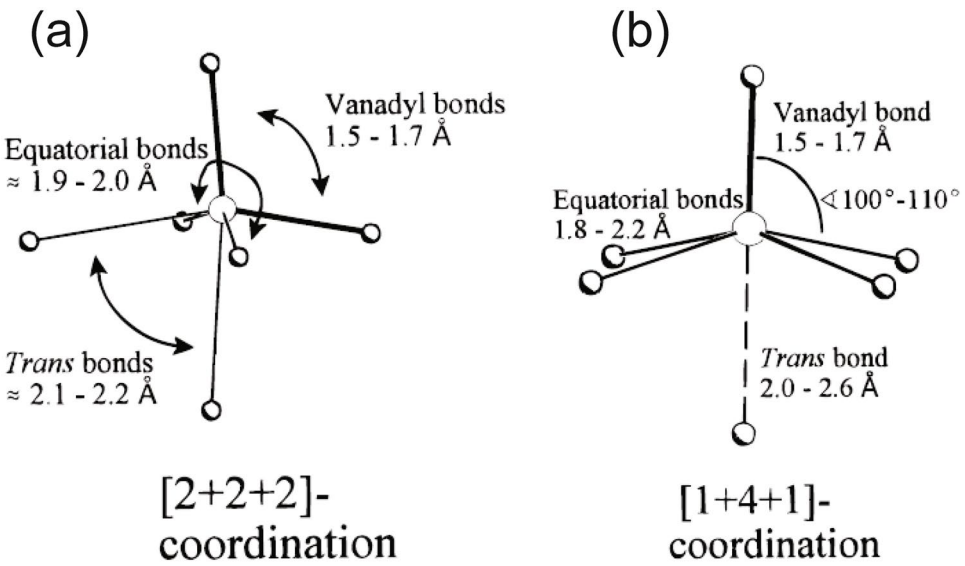

Fig. 6 Coordination geometries in ($V–O_6$) octahedra: **a** [1 + 4 + 1]-coordination with one vanadyl bond, four equatorial bonds, and one *trans* bond in a *trans* arrangement to the vanadyl bond; **b** [2 + 2 + 2]-coordination with two *cis* vanadyl bonds, two equatorial bonds, and two *trans* bonds in a *trans* arrangement to each vanadyl bond; modified after Schindler et al. (2000a, b)

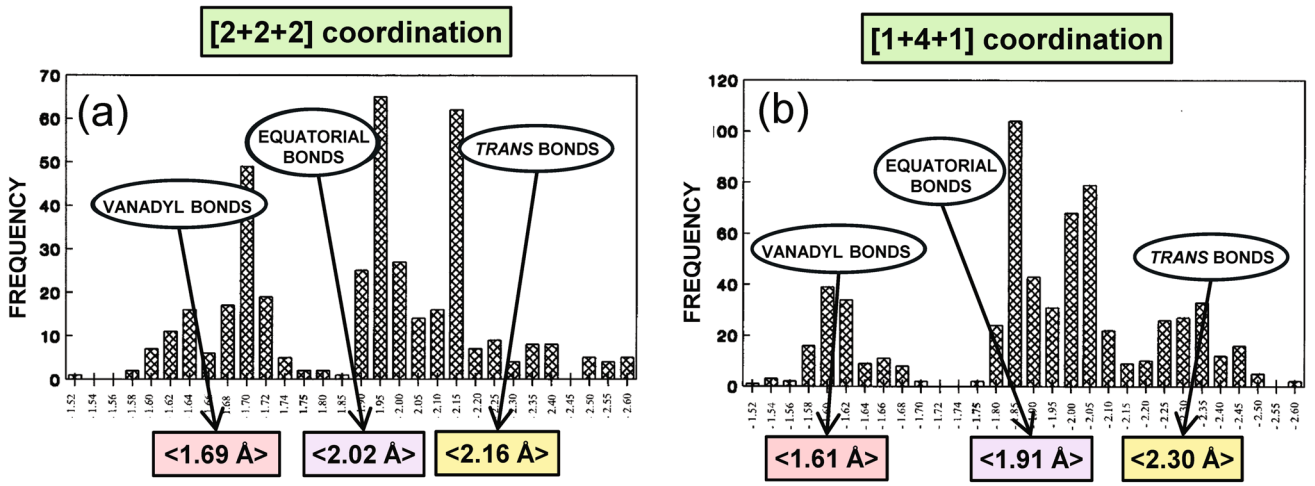

Fig. 7 Variation in V^{5+}–O^{2-} bond lengths: **a** [2 + 2 + 2] coordination; **b** [1 + 4 + 1] coordination; modified after Schindler et al. (2000a) check for 2000b

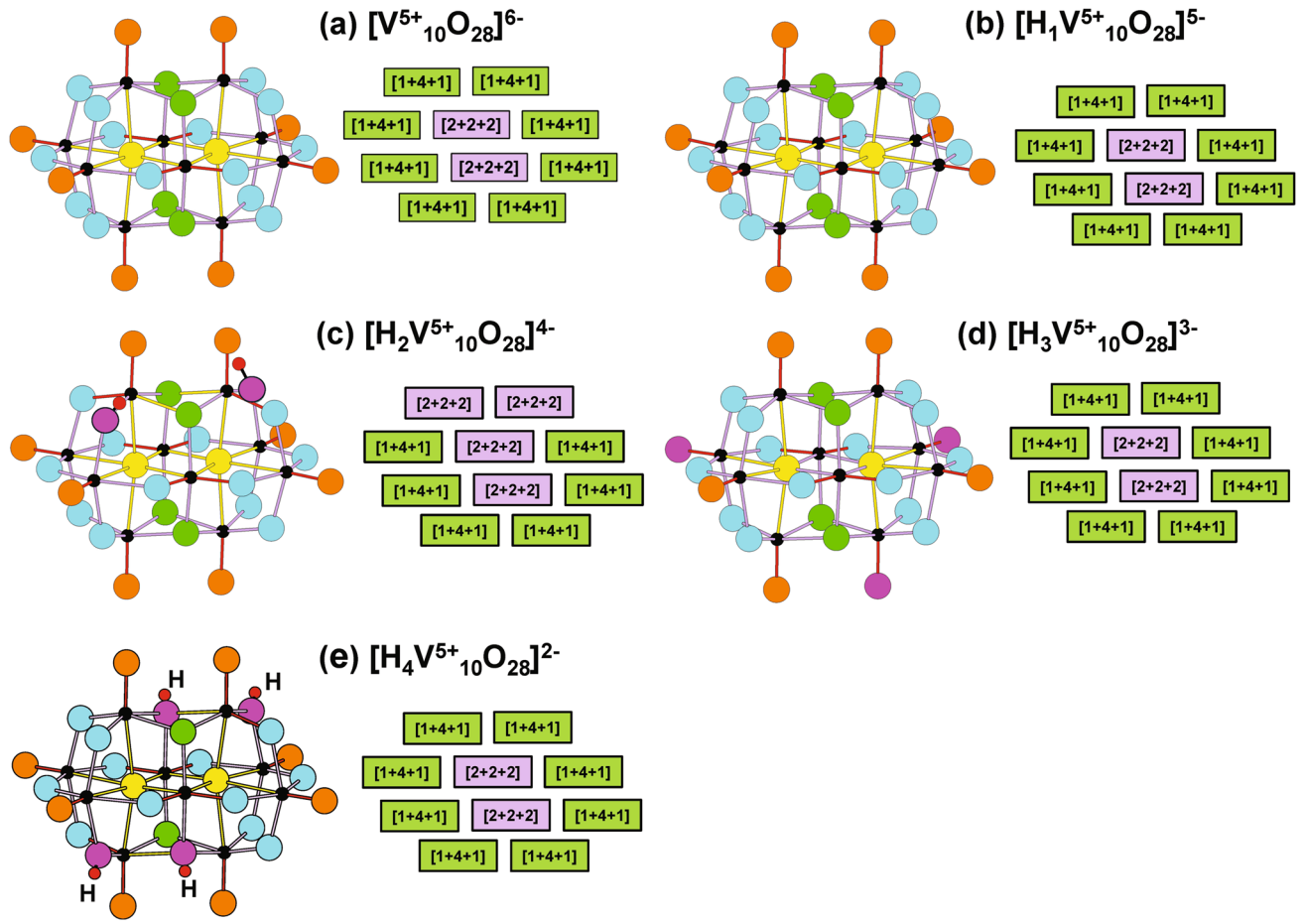

Fig. 8 **a** The $[V_{10}O_{28}]^{6-}$ decavanadate polyanion and **b**, **c**, **d**, **e** its protonated derivatives: $[H_xV^{5+}{}_{10}O_{28}]^{(6-x)-}$, x = 1–4. The patterns of [2 + 2 + 2]- and [1 + 4 + 1]-octahedra are also shown; O atoms of OH groups are shown as fuchsia circles

they are completely surrounded by V^{5+} ions and cannot bond to any ions external to the decavanadate group. In addition, there are four [3]-coordinated O^{2-} ions (shown in green), fourteen [2]-coordinated O^{2-} ions (shown in blue), and eight [1]-coordinated O^{2-} ions (shown in brown) (Fig. 2). Note that because of differences in symmetry, there cannot be a consistent labelling of the ions in the decavanadate group, and here I use the colour scheme of Fig. 2 to indicate only the topological commonalities of the different O^{2-} ions in the different decavanadate groups.

5.2 The decorated $[V^{5+}_{10}O_{28}]$ decavanadate polyanions

There are four types of decavanadate polyanions: (1) the $[V^{5+}_{10}O_{28}]^{6-}$ polyanion (see above); (2) protonated derivatives: $[H_xV^{5+}_{10}O_{28}]^{(6-x)-}$; (3) mixed-valence polyanions, both isopolyanions, e.g., $[(V^{4+}_xV^{5+}_{10-x})O_{28}]^{(6+x)-}$, and heteropolyanions, e.g., $[(Ti^{4+}_xV^{5+}_{10-x})O_{28}]^{(6+x)-}$; and (4) protonated mixed-valence polyanions, e.g., $[H^+_y(V^{4+}_xV^{5+}_{10-x})O_{28}]^{(6+x)-}$. These are illustrated in Figs. 8 and 9. Note that not all of the polyanions have refined H^+ ion positions as (1) odd numbers of H^+ ions require either long-range disorder, making location more difficult, or require refinement in a non-centrosymmetric space group, or (2) location of H^+ ions can be difficult where there is disorder in the other constituents of the structure. The arrangements of [2 + 2 + 2] and [1 + 4 + 1] octahedra are also shown for the different types (Figs. 8 and 9). All polyanions in Fig. 8 have two central [2 + 2 + 2] octahedra, and all except $[H_2V^{5+}_{10}O_{28}]^{4-}$ (Fig. 8c) are mantled by six [1 + 4 + 1] octahedra; $[H_2V^{5+}_{10}O_{28}]^{4-}$ has two [2 + 2 + 2] mantling octahedra that seem to be influenced by the non-centrosymmetric arrangement of H^+ ions. The mixed-valence polyanions are a little more mysterious. Trebiskyite (Fig. 9a) has an arrangement similar to most of the protonated decavanadates: two central [2 + 2 + 2] octahedra mantled by six [1 + 4 + 1] octahedra. Caseyite (Fig. 9b) has eight [2 + 2 + 2] octahedra and two peripheral *trans* [1 + 4 + 1] octahedra that are occupied by $(V^{4+}_{0.50}V^{5+}_{0.50})$ and an arrangement of the two H^+ ions different from that in $[H_2V^{5+}_{10}O_{28}]^{4-}$ (Fig. 8c). It is apparent that we do not yet have a complete understanding of the factors governing the arrangements of [2 + 2 + 2] and [1 + 4 + 1] octahedra in the decavanadate polyanions. However, it is also apparent that the polyanions of the decavanadate group are extremely flexible in their arrangements of chemical bonds of different strengths, promoting linkage with a wide range of interstitial complexes.

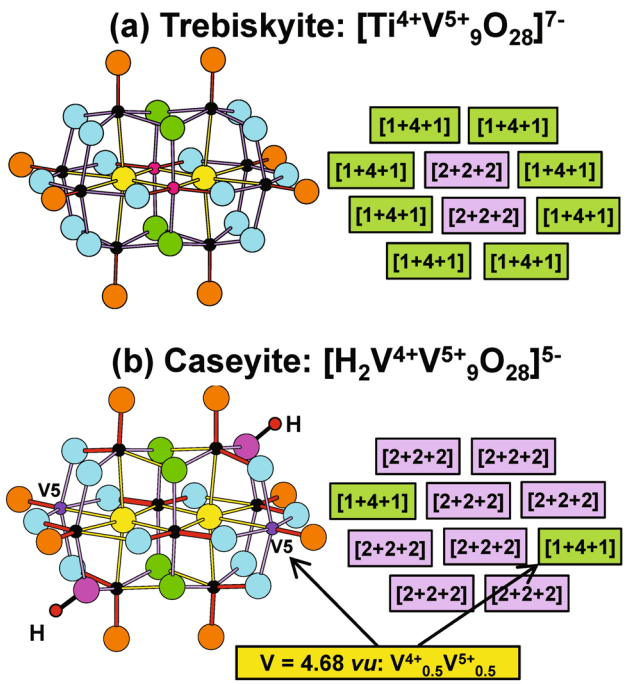

Fig. 9 Decavanadate heteropolyanions **a** $[(Ti^{4+}V^{5+}_9)O_{28}]^{7-}$ in trebiskyite, and protonated mixed-valence polyanions, **b** $[H_2(V^{4+}V^{5+}_9)O_{28}]^{5-}$ in caseyite; the V sites labelled V5 are long-range occupied by $V^{4+}_{0.5}V^{5+}_{0.5}$

6 The Lewis basicities of decavanadate groups sensu lato

Hawthorne and Schindler (2008) give details of how to calculate Lewis acid and base strengths. As a structure must be electroneutral, the bonds to the structural unit must neutralize the charge of the structural unit. The Lewis basicity of the structural unit is the effective charge on the structural unit divided by the number of bonds to the structural unit, and to calculate the Lewis basicity, we need to know (1) the effective charge on the structural unit, and (2) the number of bonds incident at the structural unit from adjacent interstitial complexes and neighboring structural units. For structural units with no H^+ ions, e.g., $[V_{10}O_{28}]^{6-}$, the effective charge on the structural unit is the formal charge. For structural units containing H^+ ions, it is necessary to account for the charge transferred from the structural unit by hydrogen bonds to external anions (commonly 0.20 *vu*; Brown 2016; Hawthorne 1992). Thus for the four types of decavanadate polyanion, we may express the effective charge as follows:

1. $[V_{10}O_{28}].^{6-}$ Effective charge = –6
2. $[H_yV_{10}O_{28}]^{(6-y)-}$ Effective charge = –6 + y–0.20y = –6 + 0.80y
3. $[(V^{4+}_xV^{5+}_{10-x})O_{28}]^{(6+x)-}$ Effective charge = –6 + x
4. $[H^+_y(V^{4+}_xV^{5+}_{10-x})O_{28}]^{(6+x)-}$ Effective charge = –6 + x + y–0.20y

Table 2 Lewis basicities for decavanadate polyanions

Polyanion	Lewis basicity (*vu*)
$[V^{5+}{}_{10}O_{28}]^{6-}$	6.0 / 52 = 0.115
$[H_1V^{5+}{}_{10}O_{28}]^{5-}$	5.2 / 52 = 0.100
$[H_2V^{5+}{}_{10}O_{28}]^{4-}$	4.4 / 52 = 0.085
$[H_3V^{5+}{}_{10}O_{28}]^{3-}$	3.6 / 52 = 0.069
$[H_4V^{5+}{}_{10}O_{28}]^{2-}$	2.8 / 52 = 0.054
$[V^{4+}{}_1V^{5+}{}_9O_{28}]^{7-}$	7.0 / 52 = 0.135
$[HV^{4+}{}_1V^{5+}{}_9O_{28}]^{6-}$	6.0 / 52 = 0.115

Calculation of the number of bonds incident at the structural unit from adjacent interstitial complexes and neighboring structural units is less straightforward for the decavanadate structures as the presence of many (often disordered) (H_2O) groups commonly precludes accurate assignment of hydrogen bonds. Earlier work (Hawthorne 1985, 1986, 1990) assumed a coordination number of [4] for O^{2-} ions in structures with pentavalent cations in a structural unit, and this value was quite successful in predicting aspects of the interstitial complex. In decavanadates, there are 28 simple anions and these need $28 \times 4 = 112$ bonds to give an anion coordination number of [4]. There are $6 \times 10 = 60$ internal bonds for $[V_{10}O_{28}]^{6-}$ and $[(V^{4+}{}_xV^{5+}{}_{10-x})O_{28}]^{(6+x)-}$, and $60 + x$ internal bonds for $[H_xV_{10}O_{28}]^{(6-x)-}$ (the additional x bonds result from the $H^+{}_x$ ions in the polyanion). In turn, the numbers of bonds required from the interstitial complex for each polyanion are as follows: $[V_{10}O_{28}]^{6-}$ and $[(V^{4+}{}_xV^{5+}{}_{10-x})O_{28}]^{(6+x)-}$: $112 - 60 = 52$; $[H_yV_{10}O_{28}]^{(6-y)-}$: $112 - 60 - y = 52 - y$. The resultant Lewis basicities for the various decavanadate polyanions are given in Table 2.

6.1 Decavanadate in aqueous solution

Decavanadates and other vanadate species are soluble in aqueous solution, forming protonic acids at near-ambient temperatures, and the stable species are very sensitive to pH (Fig. 10). All decavanadate polyanions are stable at acid pH, and we may derive the pH of maximum stability of each species from the curves in Fig. 10. Above, we calculated the Lewis basicity of each vanadate species in a very simple manner (Table 2). How do we know that these calculated values are correct? According to the principle of correspondence of Lewis acidity-basicity, the Lewis basicity of the decavanadate polyanions should correlate with the pH of the aqueous solution in which they have their maximum stability. This issue is examined in Fig. 11. The values of Lewis basicity calculated for the polyanions $[H_3V^{5+}{}_{10}O_{28}]^{3-}$, $[H_2V^{5+}{}_{10}O_{28}]^{4-}$, $[H_1V^{5+}{}_{10}O_{28}]^{5-}$ and $[V^{5+}{}_{10}O_{28}]^{6-}$ are linear with the pH values of the aqueous solutions at the maximum stabilities of these polyanions, validating our calculation of the Lewis basicities, giving confidence that these calculated values of the Lewis basicity are valid.

7 Lewis acidity-basicity and the interstitial complex

Figure 12 shows the variation in mean coordination number for simple cations (values from Gagné and Hawthorne 2017) as a function of Lewis acidity as red circles and the Lewis-base strengths for the vanadate polyanions as green circles emphasized by the dashed red ellipse. The dashed black vertical line shows the limit of the correspondence

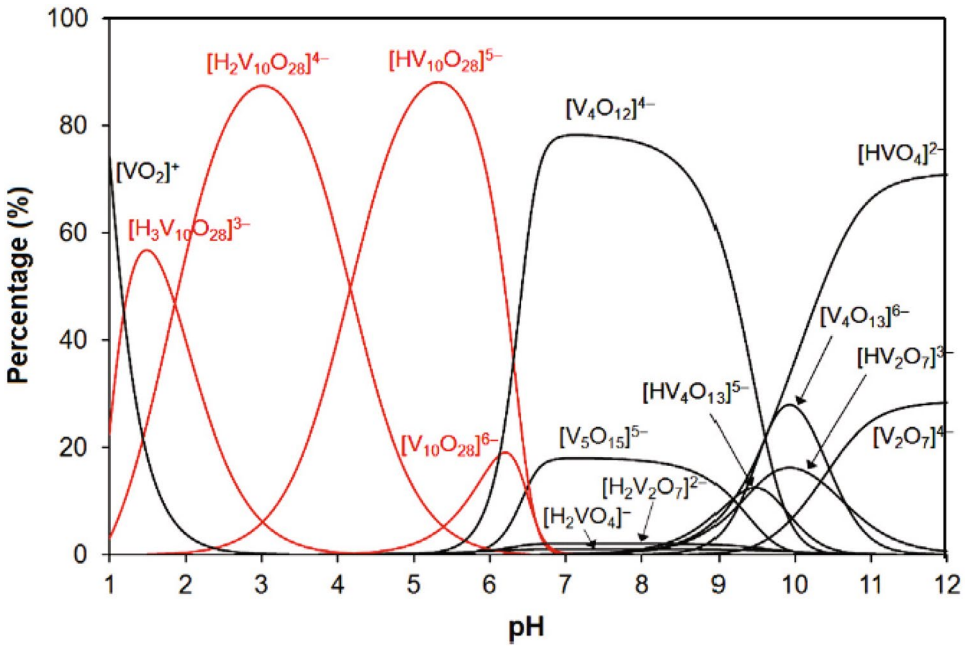

Fig. 10 Concentration of aqueous vanadate species as a function of pH at 0.200 M, with the concentrations of the decavanadate species shown in red. From Aureliano et al. (2022), copyright Elsevier

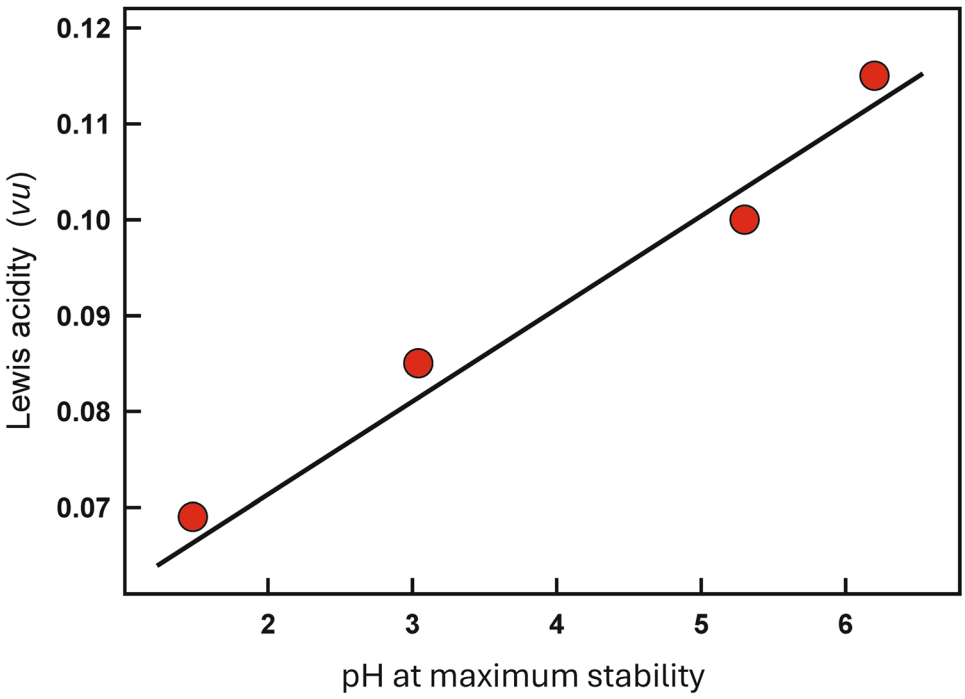

Fig. 11 Lewis acidity *versus* pH at maximum stability for decavanadate species

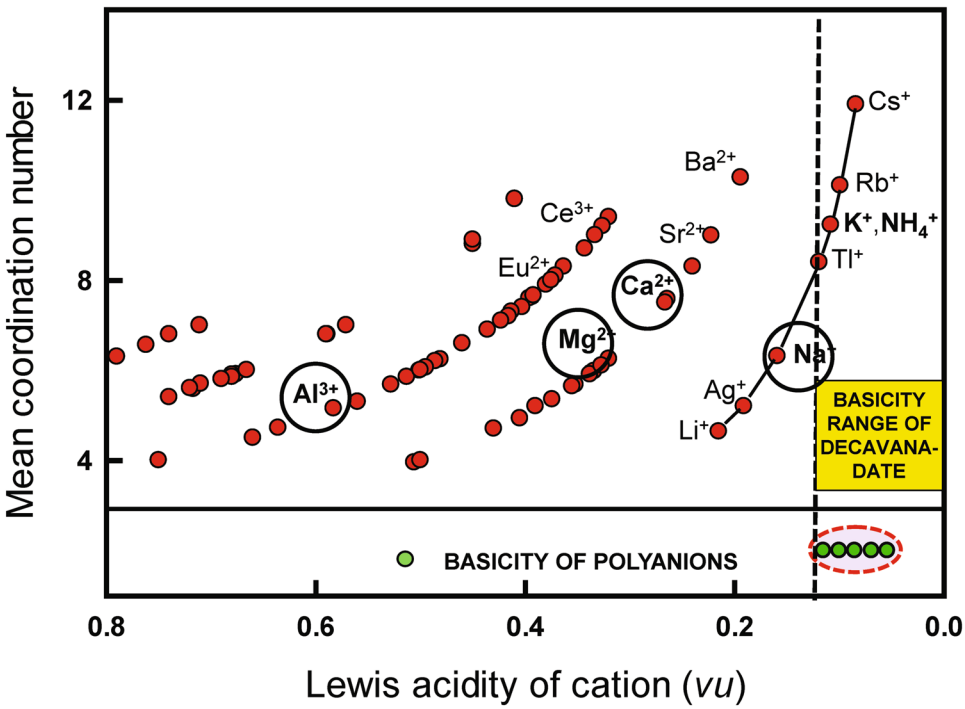

Fig. 12 Mean observed coordination number for 91 cations as a function of their Lewis acidity (red circles). The Lewis acidity for NH_4^+, 0.109 *vu* (from Hawthorne et al. 2022 from the results of García-Rodríguez et al. 2000) overlaps that of K^+, 0.110 *vu*. The green circles indicate the Lewis basicities of the decavanadate units listed in Table 2. The broken black line denotes the maximum value of the green circles

between Lewis basicity and Lewis acidity. The monovalent cations Cs^+ to Tl^+ plus $(NH_4)^+$ (Lewis acidity = 0.109 *vu*, Hawthorne et al. 2022) have Lewis acidities in the same range as the Lewis basicities of the vanadate polyanions and hence satisfy the principle of correspondence of Lewis acidity-basicity. The Lewis acidity for Na^+ lies slightly outside the range of Lewis basicity for the decavanadate polyanions. However, for simple cations, the Lewis acidity of a cation reflects the grand mean-bond-length, and a cation can decrease its effective Lewis acidity by increasing its coordination number above its average value. Na^+ has a grand mean coordination number of 6.31 (Gagné and Hawthorne 2017) and a Lewis acidity of 1/6.31 = 0.158 vu. Increasing its coordination number to [8] will change the

Lewis acidity to 1/8 = 0.125 *vu* in accord with the principle of correspondence of Lewis acidity-basicity. Thus Na^+ is the most common interstitial cation in decavanadate minerals and has coordination numbers ≥ [8]. It is apparent from Table 2 that protonated vanadate polyanions have the lowest Lewis basicities, and synthetic protonated vanadates such as $Cs_4(H_2O)_4[H_2V_{10}O_{28}]$ (Rigotti et al. 1987) and $Rb_4Na(H_2O)_{10}[HV_{10}O_{28}]$ (Yakubovich et al. 2015) contain the least-acid cations, i.e., Cs^+ and Rb^+.

Inspection of Table 1 shows that Ca^{2+}, Mg^{2+} and Al^{3+} are also common interstitial cations in decavanadate minerals and yet according to Fig. 12, their Lewis acidities lie far outside the region conforming to the principle of correspondence of Lewis acidity-basicity. How can this happen? It happens because of the presence of interstitial (H_2O) in these minerals as discussed below.

8 Transformer and non-transformer (H_2O)

(H_2O) is a very polar group: it acts as an anion on the O^{2-} side of the group and as a cation on the H^+ side of the group (Hawthorne 1992). Figure 13a shows a cation M bonding to an anion S with a bond valence of v *vu*, and Fig. 13b shows a cation M bonding to an (H_2O) group, and the (H_2O) group bonding to two anions S. In Fig. 13a, the anion receives one bond of bond valence v *vu* from the cation M. In Fig. 13b, the donor O^{2-} ion of the (H_2O) group receives a bond valence of v *vu* from the cation; the bond-valence requirements of the donor O^{2-} ion in Fig. 13b are satisfied by two short O^{2-}–H^+ bonds of strength (1 – v/2) *vu*. Each H^+ ion forms a hydrogen bond with an S anion to satisfy its own bond-valence requirements, and the S anion receives a bond valence of v/2 *vu*, one half (Fig. 13b) of what it received where it bonded directly to the M cation (Fig. 13a). The (H_2O) group is acting as a bond-valence transformer, dividing one bond into two bonds of half the

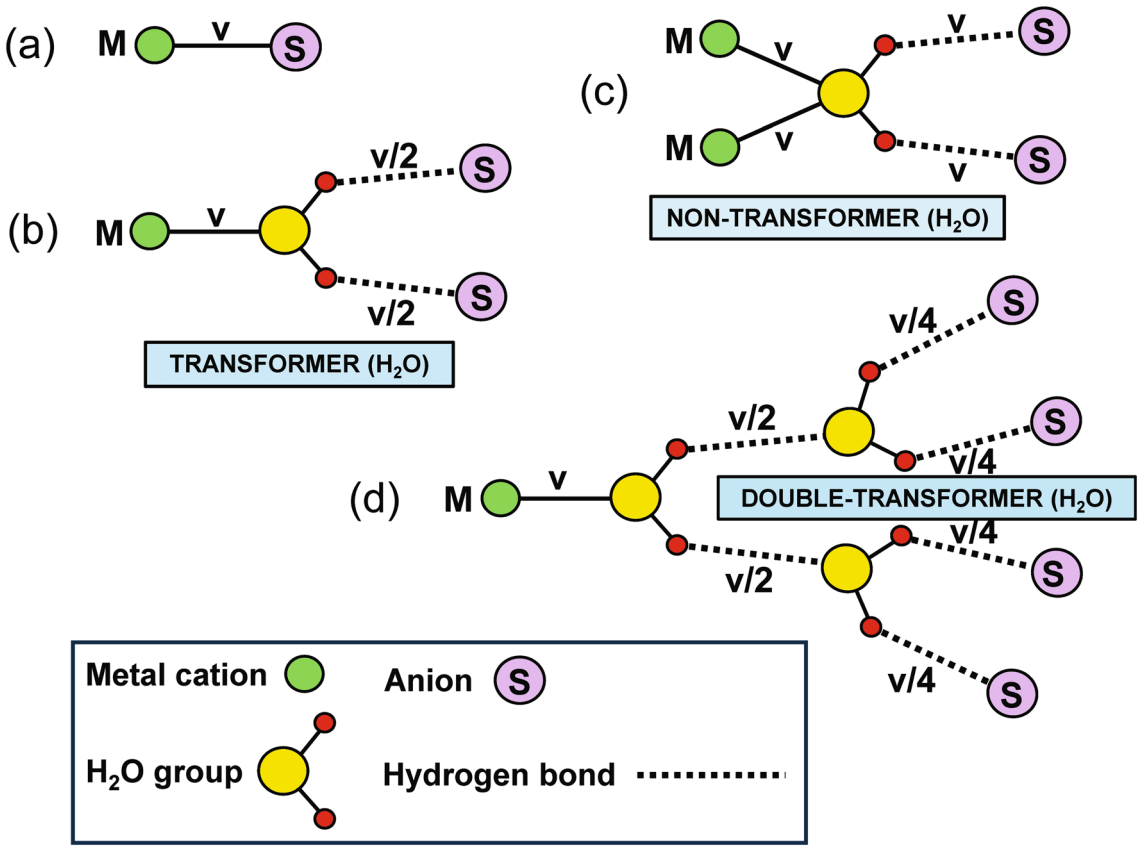

Fig. 13 The bond-valence structure around (H_2O) as a function of local bond-topology; **a** a cation, M (green) bonded to an anion, S (violet) with bond valence v *vu*; **b** a cation bonded to an (H_2O) group (O = yellow, H = red) with bond valence v *vu*; the H^+ ions hydrogen-bond to the anions S with bond valence v/2 *vu* per bond; **c** two cations bonded to an (H_2O) group with bond valence v *vu* per bond; the H^+ ions hydrogen-bond to the anions S with bond valence v *vu* per bond; **d** a cation bonded to an (H_2O) group with bond valence v *vu*; the $H.^+$ ions hydrogen-bond to other (H_2O) groups which hydrogen bonds to the anions S with bond valence v/4 *vu* per bond. Modified from Hawthorne et al. (2022)

bond valence; this type of (H_2O) group is called a *transformer (H_2O) group* (Hawthorne and Schindler 2008).

Figure 13c shows two cations bonding to an (H_2O) group, which in turn bonds to two anions. The donor O^{2-} ion receives a bond valence of 2v *vu* from the cations, and the valence-sum rule at this O^{2-} ion is satisfied by two short O–H bonds of strength (1 – v) *vu*. Each H^+ ion forms a hydrogen bond with a neighboring anion, which receives the same bond valence (v *vu*, Fig. 13c) as where it is bonded directly to one M cation (Fig. 13a); this is a *non-transformer (H_2O) group*. Figure 13d shows a cation bonding to an (H_2O) group which hydrogen bonds to two other (H_2O) groups which then hydrogen bond to four anions S. Each of the four anions S receives an incident bond-valence of v/4 *vu*, and this type of arrangement is termed a *double-transformer (H_2O) group*. The net effect of transformer and double-transformer (H_2O) groups is to allow higher-valence cations to function as interstitial constituents and yet accord with the principle of correspondence of Lewis acidity-basicity.

Table 3 Range in Lewis acidity for hydrated interstitial cations

Polyanion	Lewis basicity (*vu*)
Octahedra with transformer (H_2O) groups	
$^{[6]}M^{3+}O_{(6-n)}(H_2O)_n$	0.50–0.25
$^{[6]}M^{2+}O_{(6-n)}(H_2O)_n$	0.33–0.17
$^{[6]}M^{+}O_{(6-n)}(H_2O)_n$	0.17–0.09
Octahedra with double-transformer (H_2O) groups	
$^{[6]}M^{3+}(H_2O)_6(H_2O)_{0-12}$	0.25–0.13
$^{[6]}M^{2+}(H_2O)_6(H_2O)_{0-12}$	0.17–0.08
$^{[6]}M^{+}(H_2O)_6(H_2O)_{0-12}$	0.09–0.05

9 The stereochemistry of the interstitial complex

9.1 Simple and polyatomic cations

A *simple cation* is a single positively charged ion, e.g., Na^+, Al^{3+}, and a *polyatomic cation* is a cluster of ions with a net positive charge, e.g., $\{Na(H_2O)_6\}^+$. In the decavanadate minerals, simple cations always occur as part of a polyatomic cation. Thus in lasalite (Table 1), Na^+ has the coordination $(NaO_3(H_2O)_4)^+$ and three O^{2-} ions bond to the V^{5+} cations. However, when we write the mineral formula, the polyatomic cation does not include the bonds to the decavanadate unit and such ions are omitted from the polyatomic cation. We do not wish to lose the information of how many bonds the simple cation has with the anions of the decavanadate unit and so include the coordination number of the simple cation in the formula for the polyatomic cation: in lasalite, we write the polycation $\{^{[7]}Na(H_2O)_4\}^+$ where the difference between the coordination number of Na^+ and the number of included (H_2O) groups gives the number of bonds from Na^+ to the anions of the decavanadate unit.

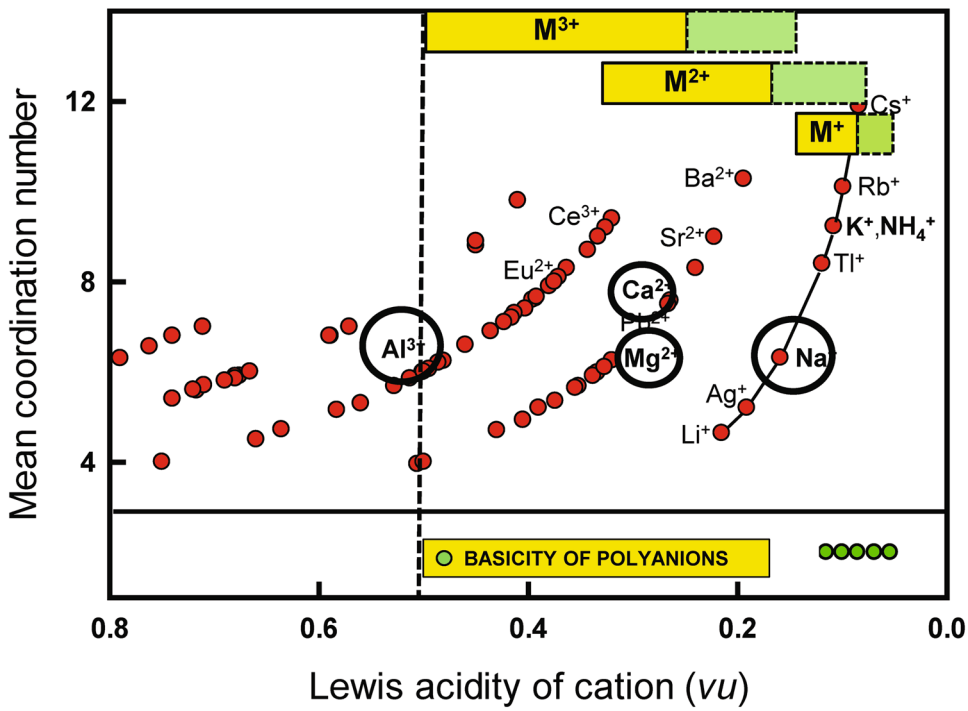

Fig. 14 Ranges in Lewis acidity of complex interstitial cations with one layer of coordinating transformer (H_2O) groups (yellow boxes) and complex interstitial cations with two layers of coordinating transformer (H_2O) groups (green boxes). The green circles indicate the Lewis basicities of the decavanadate units listed in Table 2. The broken black lines denote the maximum Lewis acidity of simple cations that can combine with (H_2O) to form complex cations that can combine with decavanadate in accord with the principle of correspondence of Lewis acidity – Lewis basicity

9.2 Transformer (H_2O) and polyatomic cations

Inspection of Fig. 12 shows that the only simple cations that obey the principle of correspondence of Lewis acidity-basicity for the decavanadate units are Cs^+, Rb^+, K^+, Tl^+ and Na^+. However, variation in the number of transformer (H_2O) groups is an effective mechanism for allowing higher-valence cations to form polyatomic cations. e.g., $\{Mg(H_2O)_6\}^{2+}$ (Fig. 13), and also obey the principle of correspondence of Lewis acidity-basicity and function as interstitial species. The Lewis acidities for hydrated interstitial cations are given in Table 3. Figure 14 indicates the range in Lewis acidity for complex cations involving mono-, di and tri-valent simple cations: yellow boxes: single transformer $M^{n+}O_m(H_2O)_{6-m}$, green boxes: double-transformer $M^{n+}(H_2O)_6(H_2O)_{12-m}$, m = 1–6. The effect of transformer (H_2O) groups is to greatly extend the range of Lewis acidity of simple interstitial cations that can form interstitial complexes that accord with the principle of correspondence of Lewis acidity-basicity.

9.3 Polymerization of polyatomic cations

Polyatomic cations rarely occur as isolated entities in the interstitial complexes of decavanadate minerals. I will just give a series of examples involving flatimers of hydrated $^{[6]}Al^{3+}$. A flatimer was defined by Kampf et al. (2022b) as a small, approximately two-dimensional Al^{3+} polyoxocation, distinguishing such arrangements from higher-symmetry Keggin-like ions such as $[AlO_4Al_{12}(OH)_{24}(H_2O)_{12}]^{7+}$ (Casey 2006). The $\{^{[6]}M^{3+}(H_2O)_6\}^{3+}$ group occurs as a monomer in hughesite (Fig. 15a), as a dimer in postite (Fig. 15b) and as a tetramer in protocaseyite (Fig. 15c). One can write a general formula for these linear flatimers as follows: $[Al_n(OH)_{2(n-1)}(H_2O)_{2(n+2)}]^{(n+2)+}$. Shared octahedron edges involve $(OH)^-$ groups and the stoichiometry of the linear polymers is not affected by staggering of the chain, as occurs in protocaseyite. If all (H_2O) groups are transformer groups, the Lewis acidity of the general $[Al_n(OH)_{2(n-1)}(H_2O)_{2(n+2)}]^{(n+2)+}$ chain is $(n+2) / 2 \times 2 \times (n+2) = 0.25$ *vu*, and the Lewis acidity of the linear flatimers is fixed: 0.25 *vu*. As the Lewis acidity of this series of linear flatimers is independent of chain length and chain configuration, the value of n and the chain configuration must be controlled by the arrangement of decavanadate units and the other constituents of the interstitial complex.

Flatimers may also be non-linear. The flatimer $[V^{5+}O_2Al_{10}(OH)_{20}(H_2O)_{18}]^{15+}$ occurs in caseyite (Fig. 15d) and $[Al_{13}(OH)_{24}(H_2O)_{24}]^{15+}$ occurs in the synthetic compound $[Al_{13}(OH)_{24}(H_2O)_{24}]Cl_{15}(H_2O)_{13}$

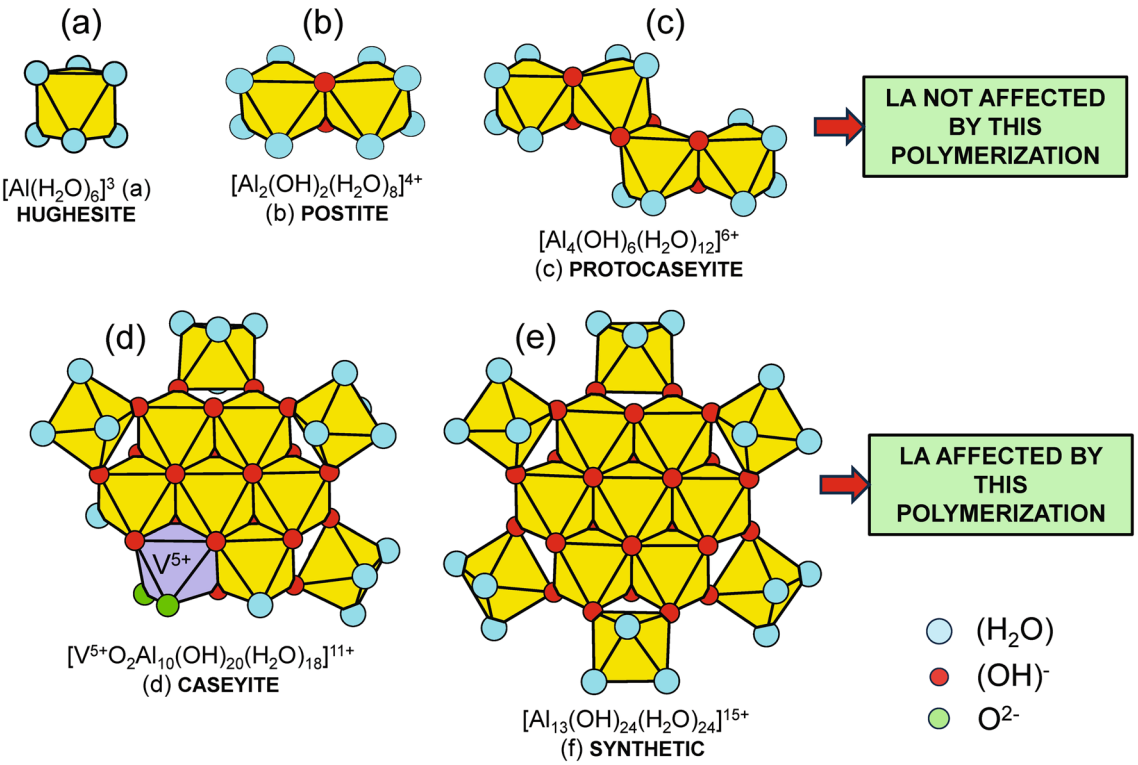

Fig. 15 Complex cations involving Al^{3+} in decavanadate minerals; **a** the monomer $[Al(H_2O)_6]^{3+}$ in hughesite; various flatimers in minerals [**b** = postite; **c** = protocaseyite; **d** = caseyite]; **e** synthetic $[Al_{13}(OH)_{24}(H_2O)_{24}]Cl_{15}(H_2O)_{13}$. Blue circles = (H_2O), red circles = $(OH)^-$, green circles = O^{2-} ions. Modified from Hawthorne et al. (2022)

(Seichter et al. 1998). The $[Al_{13}(OH)_{24}(H_2O)_{24}]^{15+}$ flatimer in caseyite has two fewer octahedra than $[Al_{13}(OH)_{24}(H_2O)_{24}]Cl_{15}(H_2O)_{13}$ (Fig. 15e) and one Al^{3+} at an edge-sharing octahedron has been replaced by V^{5+} with the loss of two H^+ ions at the outer edge, leaving two O^{2-} ions (shown in green in Fig. 15d) which receive bond-valences from V^{5+} of 1.63 and 1.59 *vu* and accept two and three hydrogen bonds, respectively. These two O^{2-} ions are hydrogen-bond acceptors whereas the other external ions of the flatimer are hydrogen-bond donors. Thus, the flatimer in caseyite has polar character, acting as a cation at most ions by donating hydrogen bonds to the structural unit and acting as an anion at the two O^{2-} anions by accepting hydrogen bonds from the structural unit.

10 Linkage between the structural unit and the interstitial complex

The decavanadate polyanion is very compact. Of the 28 simple anions, two have their bond-valence requirements satisfied by bonds within the structural unit and the remaining 26 anions have coordination numbers from [3] to [1] (Fig. 2) and present an outer anionic surface of bond-valence acceptors to their environment. The Lewis basicities of the outer O^{2-} ions vary from 0.11 to 0.34 vu (Hawthorne et al. 2022) and can receive bonds directly from interstitial cations and from H^+ ions involved in (H_2O) groups. However, as indicated by Figs. 12 and 14, the majority of the bonds from the interstitial complex to the structural unit must be hydrogen bonds. These hydrogen bonds of the interstitial (H_2O) groups are soft and compliant and impart a flexibility to the structures that allows the interstitial species to easily conform to the arrangement of the external O^{2-} ions of the decavanadate unit.

Inspection of the chemical compositions in Table 1 shows considerable variety in the chemical compositions of the interstitial complexes: some interstitial complexes have a much smaller number of individual constituents than others and the relative volumes of the structural unit and the interstitial complex can vary widely. Figure 16a and b show the structures of hughesite, $Na_3Al[V_{10}O_{28}](H_2O)_{22}$, and caseyite, $[(V^{5+}O_2)Al_{7.5}(OH)_{15}(H_2O)_{13}]_2[H_2V^{4+}V^{5+}{}_9O_{28}][V^{5+}{}_{10}O_{28}]_2(H_2O)_{90}$; the smaller volume of the interstitial complex in hughesite compared to that in caseyite is visibly apparent. The greater volume of the interstitial complex in caseyite is a result of having a large polycation, $[(V^{5+}O_2)Al_{7.5}(OH)_{15}(H_2O)_{13}]_2(H_2O)_{90}$, in its interstitial complex with a minor contribution by disordered Na^+, K^+ and Ca^{2+} ions and (SO_4) groups.

The structure of caseyite (Fig. 16b) shows the potential of the decavanadate structures to incorporate large heteropolyatomic cations into their structures. There are several large aqueous Al-hydroxide polyatomic cations (Casey 2006), including the Baker-Figgis-Keggin Al_{13}

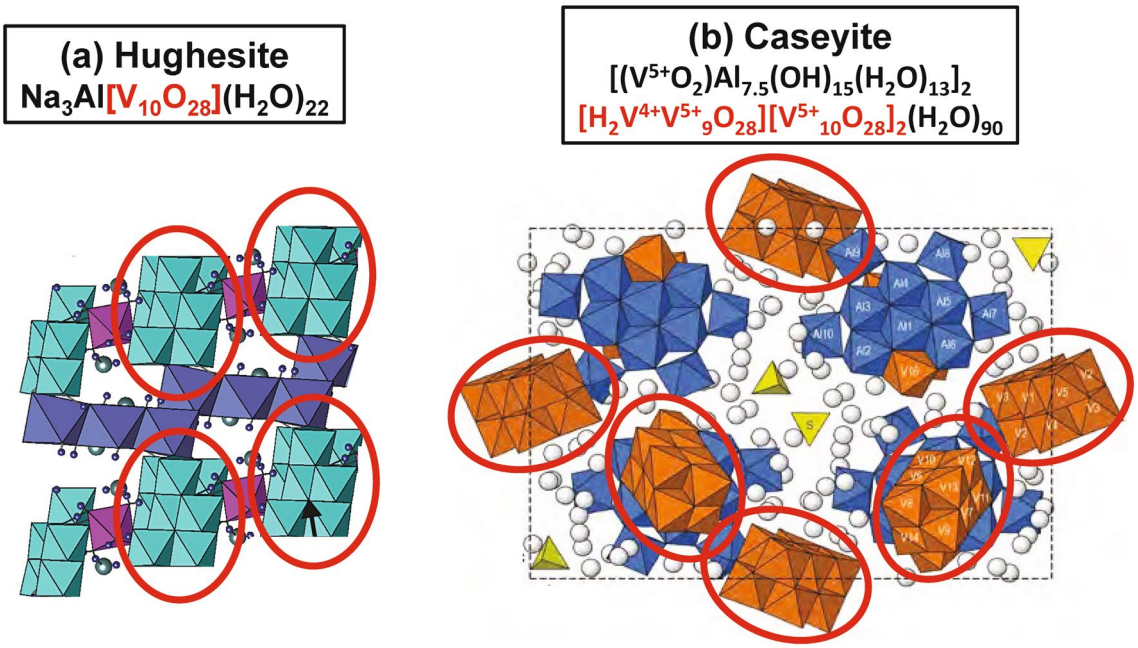

Fig. 16 The crystal structures of **a** hughesite, green = decavanadate polyanion, blue = Na polyhedral, and **b** caseyite, brown = decavanadate polyanion, blue = Al/V polycation; red ellipses outline the decavanadate polyanions in each structure. Modified from Rakovan et al. (2011) and Kampf et al. (2020a)

$[MO_4Al_{12}(OH)_{24}(H_2O)_{12}]$ isomers ($M = Ge^{4+}$, Ga^{3+} and Al^{3+}), the Al_{30} group $[Al_2O_8Al_{28}(OH)_{56}(H_2O)_{28}]^{18+}$, and various flat-$Al_n$ groups. Casey (2006) noted that "most large polymers are yet uncharacterized and unidentified…". The existence of caseyite suggests that $[V_{10}O_{28}]$ polyanions might be used to induce co-crystallization of large Al^{3+}-containing polyatomic cations from aqueous solution and lead to their structural characterization by crystal-structure solution and refinement (Hawthorne et al. 2022). Indeed, this capability of decavanadate polyanions to induce crystallization of "hard-to-crystallize" proteins is a significant feature of protein crystallography (Bijelic and Rompel 2015, 2018).

11 Proteins as giant interstitial complexes

11.1 Polyoxidometalates as protein crystallizing agents

Proteins are notoriously difficult to crystallize and this has been a significant problem in their structural characterization. Various additional constituents have been added to promote the formation of adequate crystals for structure determination. Polyoxidometallic ions are increasingly used for this purpose; they bond primarily to side chains in flexible regions of proteins and tend to reduce this flexibility to induce crystallization of good-quality crystals (e.g., Vandebroek et al. 2019). Moreover, polyoxidometallic ions have strong X-ray scattering and significantly enhance solution of the phase problem for these complex structures (e.g., Bijelic and Rompel 2018).

11.2 Polyoxidometalates as protein inhibitors

Polyoxidometalates act as inhibitors for a wide range of enzymes and are promising possible therapeutic agents for a wide range of diseases, including cancer, Alzheimer's, AIDS, diabetes and COVID-19 (e.g., Aureliano et al. 2021, 2022; Bijelic et al. 2018, 2019; Lentink et al. 2023). There is also the possibility of optimizing these inhibitory properties of specific polyoxidometalates through a better understanding of the polyoxidometalate-protein interactions.

12 Decavanadate-protein interactions

Figure 17 shows a transient receptor potential channel (TRP): a Ca^{2+}-activated cation channel permeable to Na^+ and K^+ which can modulate the operation of the cell that is important for cardiac rhythm and immune response. There are two types of decavanadate polyanions, coloured blue and brown in Fig. 17, each surrounded by red circles or rectangles. Quantitatively, the decavanadate polyanions are a very minor part of the structure, but as stated above, are instrumental in causing crystallization of the protein-decavanadate structure. Moreover, comparison of Figs. 16 and 17 emphasizes the continuum of interstitial complexes from simple alkali-metal polyhedra to polymetallic cations to proteins. Figure 18 shows the details of the bonding between the protein and the decavanadate units in which the coordination numbers of the acceptor anions of the decavanadate units are identified by the colours coded in Fig. 2. It is apparent (and not surprising) that those anions with a coordination number of [1] are the more common acceptor anions followed by those with a coordination number of [2] whereas anions with [3]- and [6]-coordination do not accept (visible) external bonds. This protein-decavanadate complex was grown at a pH of 2.0 which suggests (Fig. 10) that the decavanadate polyanion will be protonated, a factor that will significantly affect the stereochemistry of the protein-decavanadate interaction.

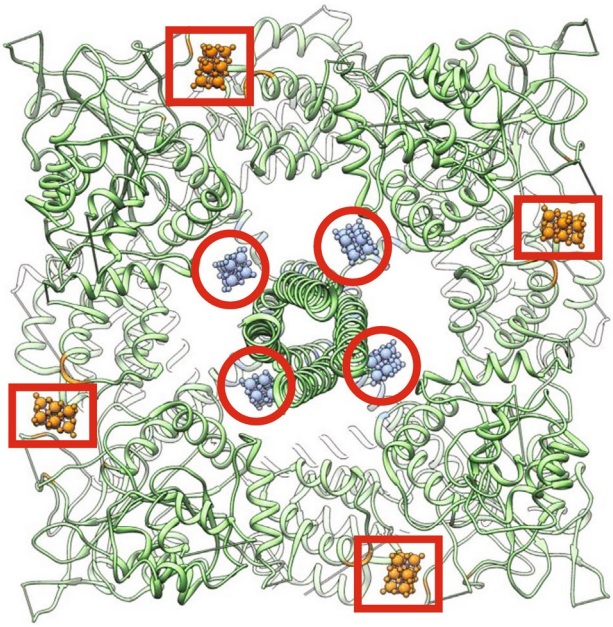

Fig. 17 Transient receptor potential channel (TRP): a Ca^{2+}-activated cation channel permeable to Na^+ and K^+ that can modulate the operation of the cell which is important for cardiac rhythm and immune response. The decavanadate units are brown and blue and are emphasized by red circles and rectangles. From Aureliano et al. (2022), copyright Elsevier

Figure 19a shows the structure of the enzyme phosphatase *Francisella tularensis*, a respiratory burst-inhibiting acid phosphatase, one of a super-family of acid phosphatases and phospholipases C (Aureliano et al. 2022), that is classified by the U.S. Centres for Disease Control and Prevention as a category A bio-terrorism agent. Figure 19b and c show the details of the bonding between the protein and the

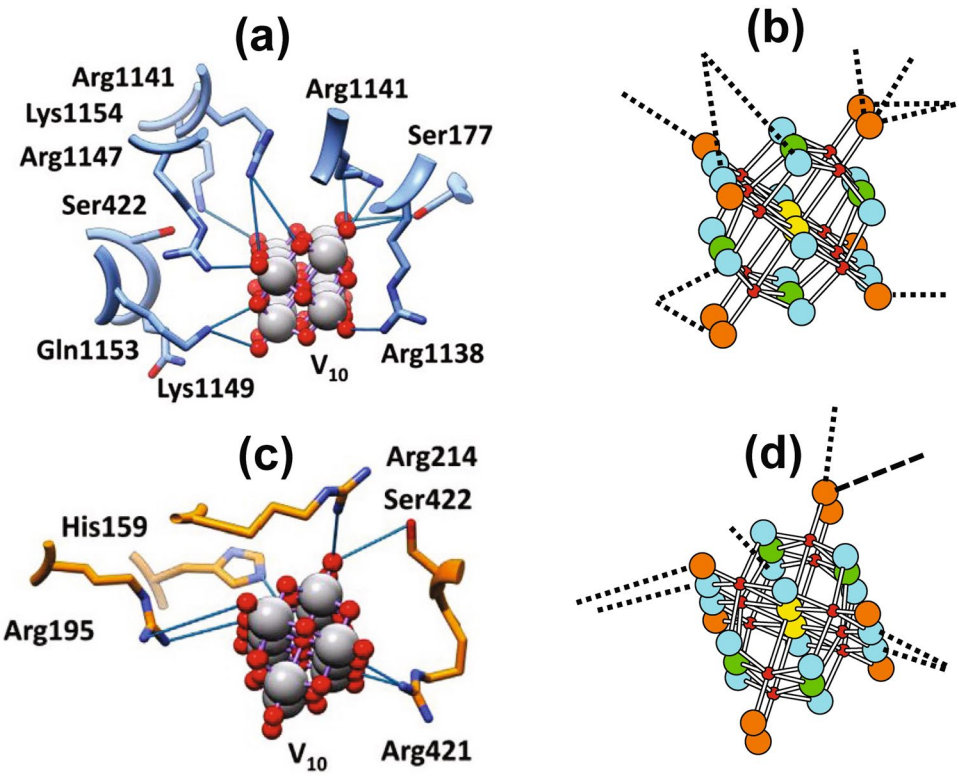

Fig. 18 **a**, **c** Details of the bonding between the decavanadate polyanions and the protein of Fig. 17 by hydrogen bonds and metal-O bonds. **b**, **d** showing the bonding to the differently coordinated O^{2-} ions in the decavanadates, colours as in Fig. 2: brown = [1], blue = [2], green = [3] and yellow = [6]. **a** and **c** are from Aureliano et al. (2022), copyright Elsevier

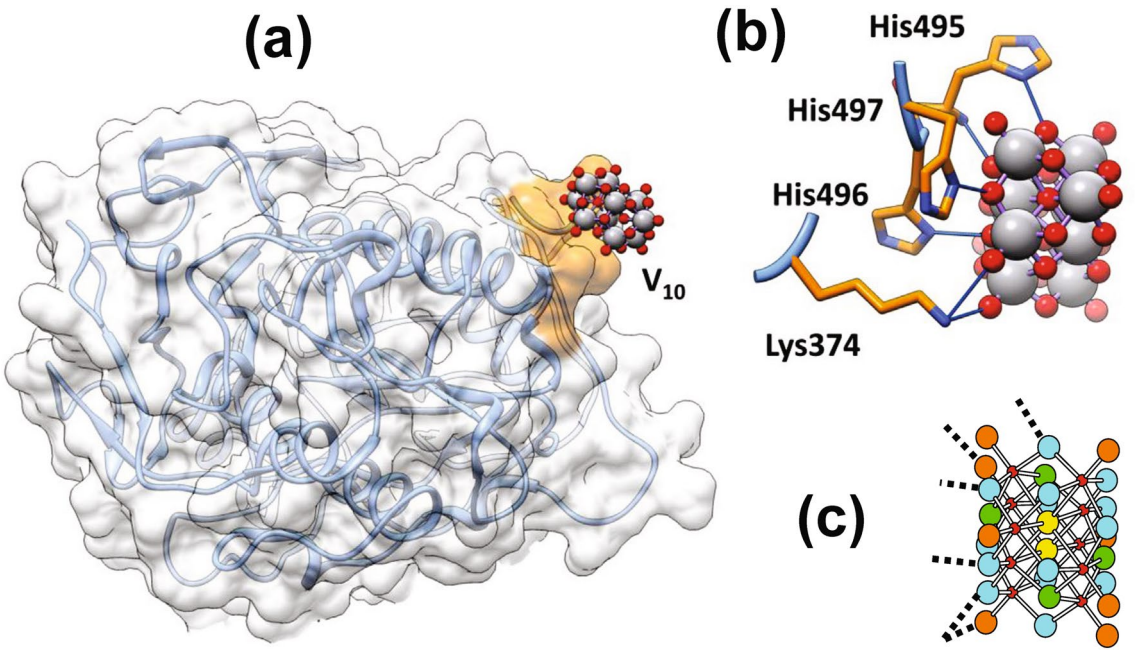

Fig. 19 **a** The structure of *Francisella tularensis* AcPA decavanadate complex; **b** interaction of the protein surface with decavanadate; **c** showing the bonding to the differently coordinated O^{2-} ions in the decavanadates, colours as in Fig. 2: brown = [1], blue = [2], green = [3] and yellow = [6]. **a** and **b** are modified from Aureliano et al. (2022), copyright Elsevier

decavanadate units in which the coordination numbers of the acceptor anions of the decavanadate are [1] and [2]. It seems worthwhile in the future to examine in more detail the stereochemical relations between the hydrogen-bond donors and the metals of the protein active sites and the acceptor anions of the decavanadate, as this may lead to increased

control and optimization of the inhibitory action(s) of the decavanadate polyanion.

13 Coda

1. The pascoite-family minerals contain decavanadate polyanions of four different types: (i) $[V^{5+}{}_{10}O_{28}]^{6-}$, (ii) mixed-valence $[(V^{4+}{}_{x}V^{5+}{}_{(10-x)}O_{28}]^{(6+x)-}$, (iii) protonated $[H^{+}{}_{y}V^{5+}{}_{10}O_{28}]^{(6-y)-}$ and (iv) protonated mixed-valence $[(H^{+}{}_{y}V^{4+}{}_{x}V^{5+}{}_{(10-x)}O_{28}]^{(6+x-y)-}$.
2. The decavanadate units form the structural units which are linked together by cations and (H_2O) of the interstitial complex.
3. Linkage between the decavanadate units and the interstitial complexes is constrained by the principle of correspondence of Lewis acidity-basicity.
4. The Lewis base strengths of the various decavanadate polyanions vary from 0.054 to 0.154 vu.
5. The principle of correspondence of Lewis acidity-basicity shows that decavanadate structures can form from simple cations only for Cs^+, Rb^+, K^+, Tl^+ and Na^+. Simple cations such as Ca^{2+}, Mg^{2+} and Al^{3+} are too acidic to form decavanadate structures by themselves.
6. Such cations may bond to transformer (H_2O) groups to form polyatomic cations that have lower Lewis acidities than the constituent simple cations.
7. The occurrence of the complex polyatomic cation $\{(V^{5+}O_2)Al_{10}(OH)_{20}(H_2O)_{18}\}^{11+}$ in caseyite shows the potential of decavanadate structures to incorporate large complex heteropolycations into their structures.
8. Decavanadates may combine with proteins to form crystals in which the proteins act as giant interstitial complexes.
9. Decavanadate can act as an inhibitor for several enzymes and are promising possible therapeutic agents for a wide range of diseases, including cancer.
10. The principle of correspondence of Lewis acidity-basicity suggests that, by changing the form of the decavanadate by altering the ambient pH and adding additional Lewis acids, it may be possible to tune the inhibitory function of the decavanadate and lead to more control of the inhibitory process.

Acknowledgements I thank Fernando Cámara and an anonymous reviewer for their perspicacious comments on this paper. This work was supported by a Discovery Grant from the Natural Sciences and Engineering Research Council of Canada to FCH.

Author contributions I am the sole author and contributor to this manuscript.

Funding Natural Sciences and Engineering Research Council of Canada.

Data availability No datasets were generated or analysed during the current study.

Declarations

Conflict of interest The author declares no conflicts of interest.

References

Angel RJ, Gatta D, Boffa Ballaran T, Carpenter MA (2008) The mechanism of coupling in the modulated structure of nepheline. Can Mineral 46:1465–1476

Aureliano M, Gumerova NI, Sciortino G, Garribba E, Rompel A, Crans DE (2021) Polyoxovanadates with emerging biomedical activities. Coord Chem Rev 447:214143

Aureliano M, Gumerova MNI, Sciortino G, Garribba E, McLauchlan CC, Rompel A, Crans DC (2022) Polyoxidovanadates' interactions with proteins: an overview. Coord Chem Rev 454:214344

Bijelic A, Rompel A (2015) The use of polyoxometalates in protein crystallography - an attempt to widen a well-known bottleneck. Coord Chem Rev 299:22–38

Bijelic A, Rompel A (2018) Polyoxometalates: more than a phasing tool in protein crystallography. Chem Texts 4:10

Bijelic A, Aureliano M, Rompel A (2018) The antibacterial activity of polyoxometalates: structures, antibiotic effects and future perspectives. Chem Comm 54:1153–1169

Bijelic A, Aureliano M, Rompel A (2019) Polyoxometalates as potential next-generation metallodrugs in the combat against cancer. Angew Chem Int Ed 58:2980–2999

Brown ID (2009) Recent developments in the methods and applications of the bond valence model. Chem Rev 109:6858–6919

Brown ID (2016) The chemical bond in inorganic chemistry. The bond valence model. Oxford University Press, UK

Carter WD, Gualtieri JL (1965) Geology and uranium–vanadium deposits of the La Sal quadrangle, San Juan County, Utah, and Montrose County, Colorado. US Geol Survey Prof Pap 508

Casey WH (2006) Large aqueous aluminum hydroxide molecules. Chem Rev 106:1–16

Colombo F, Baggio R, Kampf AR (2011) The crystal structure of the elusive huemulite. Can Mineral 49:849–864

Cooper MA, Hawthorne FC, Kampf AR, Hughes JM (2019a) Determination of V^{4+}:V^{5+} ratios in the $[V_{10}O_{28}]^{n-}$ decavanadate polyanion. Can Mineral 57:235–244

Cooper MA, Hawthorne FC, Kampf AR, Hughes JM (2019b) Identifying protonated decavanadate polyanions. Can Mineral 57:245–253

Evans HT Jr (1966) The molecular structure of the isopoly complex ion, decavanadate ($V_{10}O_{28}{}^{6-}$). Contrib US Geol Surv 5:967–977

Gagné OC, Hawthorne FC (2016) Bond-length distributions for ions bonded to oxygen: alkali and alkaline-earth metals. Acta Crystallogr B 72:602–625

Gagné OC, Hawthorne FC (2017) Empirical Lewis-acid strengths for 135 cations bonded to oxygen. Acta Crystallogr B 73:956–961

Gagné OC, Hawthorne FC (2018a) Bond-length distributions for ions bonded to oxygen: Metalloids and post-transition metals. Acta Crystallogr B 74:63–78

Gagné OC, Hawthorne FC (2018b) Bond-length distributions for ions bonded to oxygen: results for the non-metals and discussion of lone-pair stereoactivity and the polymerization of PO_4. Acta Crystallogr B 74:79–96

Gagné OC, Hawthorne FC (2020) Bond-length distributions for ions bonded to oxygen: Results for the transition metals and quantification of the factors underlying bond-length variation in inorganic solids. IUCrJ 7:581–629

García-Rodríguez L, Rute-Pérez Á, Piñero JR, González-Silgo C (2000) Bond-valence parameters for ammonium-anion interactions. Acta Crystallogr B 56:565–569

Gordillo CE, Linares E, Toubes RO, Winchell H (1966) Huemulite, $Na_4MgV_{10}O_{28}{\cdot}24H_2O$, a new hydrous sodium and magnesium vanadate from Huemul mine, Mendoza Province, Argentina. Am Mineral 51:1–13

Hawthorne FC (1983) Graphical enumeration of polyhedral clusters. Acta Crystallogr A 39:724–736

Hawthorne FC (1985) Towards a structural classification of minerals: The $^{VI}M^{IV}T_2\varphi_n$ minerals. Am Mineral 70:455–473

Hawthorne FC (1986) Structural hierarchy in $^{VI}M_x{}^{III}T_y\varphi_z$ minerals. Can Mineral 24:625–642

Hawthorne FC (1990) Structural hierarchy in $^{[6]}M^{[4]}T\varphi_n$ minerals. Z Kristallogr 192:1–52

Hawthorne FC (1992) The role of OH and H_2O in oxide and oxysalt minerals. Z Kristallogr 201:183–206

Hawthorne FC (1994) Structural aspects of oxides and oxysalt crystals. Acta Crystallogr B 50:481–510

Hawthorne FC (2012) A bond-topological approach to theoretical mineralogy: crystal structure, chemical composition and chemical reactions. Phys Chem Mineral 39:841–874

Hawthorne FC (2014) The structure hierarchy hypothesis. Mineral Mag 78:957–1027

Hawthorne FC (2015) Toward theoretical mineralogy: a bond-topological approach. Am Mineral 100:696–713

Hawthorne FC (2018) A bond-topological approach to borate minerals: A brief review. Phys Chem Glasses–eur J Glass Sci Tech Part B 59:121–129

Hawthorne FC, Ferguson RB (1975) Anhydrous sulphates. I. Refinement of the crystal structure of celestite, with an appendix on the structure of thenardite. Can Mineral 13:181–187

Hawthorne FC, Gagné OC (2024) New ion radii for oxides and oxysalts, fluorides, chlorides and nitrides. Acta Crystallogr B 80:326–339

Hawthorne FC, Schindler M (2008) Understanding the weakly bonded constituents in oxysalt minerals. Z Kristallogr 223:41–68

Hawthorne FC, Hughes JM, Cooper MA, Kampf AR (2022) Bonding between the decavanadate polyanion and the interstitial complex in pascoite-family minerals. Can Mineral 60:341–359

Hillebrand WF, Merwin HE, Wright FE (1914) Hewettite, metahewettite and pascoite, hydrous calcium vanadates. Proc Am Philos Soc 53(213):31–54

Hughes JM, Schindler M, Rakovan J, Cureton FE (2002) The crystal structure of hummerite, $KMg(V_5O_{14}){\cdot}8H_2O$: bonding between the $[V_{10}O_{28}]^{6-}$ structural unit and the $\{K_2Mg_2(H_2O)_{16}\}^{6+}$ interstitial complex. Can Mineral 40:1429–1435

Hughes JM, Schindler M, Francis CA (2005) The C2/m disordered structure of pascoite, $Ca_3(V_{10}O_{28}){\cdot}17H_2O$. Can Mineral 43:1379–1386

Hughes JM, Wise WS, Gunter ME, Morton JP, Rakovan J (2008) Lasalite, $Na_2Mg_2[V_{10}O_{28}]{\cdot}20H_2O$, a new decavanadate mineral species from the Vanadium Queen Mine, La Sal District, Utah: description, atomic arrangement, and relationship to the pascoite group of minerals. Can Mineral 46:1365–1372

Kampf AR, Steele IM (2008) Magnesiopascoite, a new member of the pascoite group: description and crystal structure. Can Mineral 46:679–686

Kampf AR, Hughes JM, Marty J, Nash B (2011a) Gunterite, $Na_4(H_2O)_{16}(H_2V_{10}O_{28}){\cdot}6H_2O$, a new mineral with a doubly-protonated decavanadate polyanion: crystal structure and descriptive mineralogy. Can Mineral 49:1243–1251

Kampf AR, Hughes JM, Marty J, Gunter ME, Nash B (2011b) Rakovanite, $Na_3\{H_3[V_{10}O_{28}]\}{\cdot}15H_2O$, a new species of the pascoite family with a protonated decavanadate polyanion. Can Mineral 49:595–604

Kampf AR, Hughes JM, Marty J, Nash B (2012) Postite, $Mg(H_2O)_6Al_2(OH)_2(H_2O)_8(V_{10}O_{28}){\cdot}13H_2O$, a new mineral species from the La Sal mining district, Utah: Crystal structure and descriptive mineralogy. Can Mineral 50:45–53

Kampf AR, Hughes JM, Marty J, Nash B (2013a) Wernerbaurite, $\{[Ca(H_2O)_7]_2(H_2O)_2(H_3O)_2\}\{V_{10}O_{28}\}$, and schindlerite, $\{[Na_2(H_2O)_{10}](H_3O)_4\}\{V_{10}O_{28}\}$, the first hydronium-bearing decavanadate minerals. Can Mineral 51:297–312

Kampf AR, Hughes JM, Marty J, Brown FH (2013b) Nashite, $Na_3Ca_2([V^{5+}{}_9V^{4+}{}_1]O_{28}){\cdot}24H_2O$, a new mineral species from the Yellow Cat Mining District, Utah and the Slick Rock Mining District, Colorado: Crystal structure and descriptive mineralogy. Can Mineral 51:27–37

Kampf AR, Hughes JM, Nash BP, Marty J (2014a) Kokinosite, $Na_2Ca_2(V_{10}O_{28}){\cdot}24H_2O$, a new decavanadate mineral species from the St. Jude mine, Colorado: crystal structure and descriptive mineralogy. Can Mineral 52:15–25

Kampf AR, Hughes JM, Marty J, Nash BP, Chen Y-S, Steele IM (2014b) Bluestreakite, $K_4Mg_2(V^{4+}{}_2V^{5+}{}_8O_{28}){\cdot}14H_2O$, a new mixed-valence decavanadate mineral from the Blue Streak Mine, Montrose County, Colorado: crystal structure and descriptive mineralogy. Can Mineral 52:1007–1018

Kampf AR, Hughes JM, Nash BP, Marty J, Cooper MA, Hawthorne FC, Karpenko VY, Pautov LA, Agakhanov AA (2016) Revision of the formulas of wernerbaurite and schindlerite: Ammonium- rather than hydronium-bearing decavanadate minerals. Can Mineral 54:555–558

Kampf AR, Nash BP, Marty J, Hughes JM (2017a) Burroite, $Ca_2(NH_4)_2(V_{10}O_{28}){\cdot}15H_2O$, a new decavanadate mineral from the Burro mine, San Miguel County, Colorado. Can Mineral 55:473–481

Kampf AR, Nash BP, Marty J, Hughes JM, Rose TP (2017b) Hydropascoite, $Ca_3(V_{10}O_{28}){\cdot}24H_2O$, a new decavanadate mineral from the Packrat mine, Mesa County, Colorado. Can Mineral 55:207–217

Kampf AR, Nash BP, Adams PM, Marty J, Hughes JM (2018) Ammoniolasalite, $[(NH_4)_2Mg_2(H_2O)_{20}][V_{10}O_{28}]$, a new decavanadate species from the Burro mine, Slick Rock district, Colorado. Can Mineral 56:859–869

Kampf AR, Cooper MA, Hughes JM, Nash BP, Hawthorne FC, Marty J (2020a) Caseyite, a new mineral containing a variant of the flat-Al_{13} polyoxometalate cation. Am Mineral 105:123–131

Kampf AR, Adams PM, Nash BP, Marty J, Hughes JM (2020b) Okieite, $Mg_3[V_{10}O_{28}]{\cdot}28H_2O$, a new decavanadate mineral from the Burro mine, Slick Rock district, San Miguel County, Colorado, USA. Can Mineral 58:125–135

Kampf AR, Hughes JM, Cooper MA, Hawthorne FC, Nash BP, Olds TA, Adams PM, Marty J (2021) The pascoite family of minerals, including the redefinition of rakovanite. Can Mineral 59:771–779

Kampf AR, Cooper MA, Hawthorne FC, Hughes JM, Nash BP, Adams PM (2022a) Redefinition of gunterite. Can Mineral 60:361–368

Kampf AR, Cooper MA, Hughes JM, Ma C, Hawthorne FC, Casey WH, Marty J (2022b) Protocaseyite, a new decavanadate mineral containing a $[Al_4(OH)_6(H_2O)_{12}]^{6+}$ linear tetramer, a novel isopolycation. Am Mineral 107:1181–1189

Katsoulis DE (1998) A survey of applications of polyoxometalates. Chem Rev 98:359–387

Lentink S, Salazar Marcano DE, Aly Moussawi M, Parac-Vogt TN (2023) Exploiting interactions between polyoxometalates and proteins for applications in (bio)chemistry and medicine. Agnew Chem Int Ed 62:e202303817

Olds TA, Kampf AR, Cooper MA, Adams PM, Marty J (2024) Trebiskyite, the first titanium-decavanadate mineral. Can J Mineral Petrol 62:117–132

Rakovan J, Schmidt GR, Gunter M, Nash B, Kampf AR, Marty J, Wise WS (2011) Hughesite, $Na_3Al(V_{10}O_{28})\cdot 22H_2O$, a new member of the pascoite family of minerals from the Sunday mine, San Miguel County, Colorado. Can Mineral 49:1253–1265

Rigotti G, Rivero BE, Castellano EE (1987) The pseudo-orthorhombic structure of cesium dihydrogendecavanadate tetrahydrate. Acta Crystallogr C 43:197–201

Schindler M, Hawthorne FC (2001a) A bond-valence approach to the structure, chemistry and paragenesis of hydroxy-hydrated oxysalt minerals: I. Theory Can Mineral 39:1225–1242

Schindler M, Hawthorne FC (2001b) A bond-valence approach to the structure, chemistry and paragenesis of hydroxy-hydrated oxysalt minerals: II. crystal structure and chemical composition of borate minerals. Can Mineral 39:1243–1256

Schindler M, Hawthorne FC (2008) The stereochemistry and chemical composition of interstitial complexes in uranyl-oxysalt minerals. Can Mineral 46:467–501

Schindler M, Hawthorne FC, Baur WH (2000a) Crystal-chemical aspects of vanadium: Polyhedral geometries, characteristic bond valences and polymerization of (VO_n) polyhedra. Chem Mater 12:1248–1259

Schindler M, Hawthorne FC, Baur WH (2000b) A crystal-chemical approach to the composition and occurrence of vanadium minerals. Can Mineral 38:1443–1456

Seichter W, Moegel HJ, Brand P, Salah D (1998) Crystal structure and formation of the aluminum hydroxide chloride $[Al_{13}(OH)_{24}(H_2O)_{24}]Cl_{15}\times 13(H_2O)$. Eur J Inorg Chem 1998:795–797

Shawe DR (2011) Uranium-vanadium deposits of the Slick Rock district. Colorado. US Geol Surv Prof Pap 576:80

Tait KT, Sokolova EV, Hawthorne FC, Khomyakov AP (2003) The crystal chemistry of nepheline. Can Mineral 41:61–70

Vandebroek L, Mampaey Y, Antonyuk S, Van Meervelt L, Parac-Vogt TN (2019) Noncovalent complexes formed between metal-substituted polyoxometalates and hen egg white lysozyme. Eur J Inorg Chem 2019:506–511

Weeks AD, Cisney EA, Sherwood AM (1951) Hummerite and montroseite, two vanadium minerals from Montrose County, Colorado. Am Mineral 36:326–327

Yakubovich OV, Steele IM, Yakovleva EV, Dimitrova OV (2015) One-dimensional decavanadate chains in the crystal structure of $Rb_4[Na(H_2O)_6][HV_{10}O_{28}]\cdot 4H_2O$. Acta Crystallogr C 71:465–473